NASA TECHNICAL MEMORANDUM

NASA TM X-3105

DIGITAL IMPLEMENTATION OF THE TF30-P-3 TURBOFAN ENGINE CONTROL

David S. Cwynar and Peter G. Batterton

Lewis Research Center

Cleveland, Ohio 44135

NATIONAL AERONAUTICS AND SPACE ADMINISTRATION • WASHINGTON, D. C. • FEBRUARY 1975

1. Report No. NASA TM X-3105	2. Government Accession No.	3. Recipient's Catalog No.
4. Title and Subtitle DIGITAL IMPLEMENTATION OF THE TF30-P-3 TURBOFAN ENGINE CONTROL		5. Report Date February 1975
		6. Performing Organization Code
7. Author(s) by David S. Cwynar and Peter G. Batterton		8. Performing Organization Report No. E-8064
9. Performing Organization Name and Address Lewis Research Center National Aeronautics and Space Administration Cleveland, Ohio 44135		10. Work Unit No. 501-24
		11. Contract or Grant No.
12. Sponsoring Agency Name and Address National Aeronautics and Space Administration Washington, D.C. 20546		13. Type of Report and Period Covered Technical Memorandum
		14. Sponsoring Agency Code

15. Supplementary Notes

16. Abstract

The standard hydromechanical control modes for TF30-P-3 engine were implemented on a digital process control computer. Programming methods are described, and a method is presented to solve stability problems associated with fast response dynamic loops contained within the exhaust nozzle control. In addition a modification of the exhaust nozzle control to provide for either velocity or position servoactuation systems is discussed. Transient response of the digital control was evaluated by tests on a real time hybrid simulation of the TF30-P-3 engine. It is shown that the deadtime produced by the calculation time delay between sampling and final output is more significant to transient response than the effects associated with sampling rate alone. For the main fuel control, extended update and calculation times resulted in a lengthened transient response to throttle bursts from idle to intermediate with an increase in high pressure compressor stall margin. Extremely long update intervals of 250 msec could be achieved without instability. Update extension for the exhaust nozzle control resulted in a delayed response of the afterburner light-off detector and exhaust nozzle overshoot with resulting fan oversupression. Long update times of 150 msec caused failure of the control due to a false indication by the blowout detector.

17. Key Words (Suggested by Author(s)) Digital control Propulsion control Engine control Airbreathing propulsion	18. Distribution Statement Unclassified - unlimited STAR category 07 (rev.)		
19. Security Classif. (of this report) Unclassified	20. Security Classif. (of this page) Unclassified	21. No. of Pages 54	22. Price* $3.75

* For sale by the National Technical Information Service, Springfield, Virginia 22151

DIGITAL IMPLEMENTATION OF THE TF30-P-3

TURBOFAN ENGINE CONTROL

by David S. Cwynar and Peter G. Batterton

Lewis Research Center

SUMMARY

The design of a digital control for the TF30-P-3 engine is described with detailed flow charts and programming methods. The control is designed to duplicate the existing hydromechanical control modes over the entire operating range. The control was implemented on a general purpose process control computer and required 4833 words of storage and a 3.23-msec calculation time. Transient response of the digital control was evaluated by tests on a real time hybrid simulation of the TF30-P-3 engine.

It is shown that the deadtime produced by the calculation time delay between sampling and final output is more significant to transient response than the effects associated with sampling rate alone. Transient response deterioration of the main fuel control limited update times to 75 msec for a 3.23-msec calculation time, and to 20 msec for a 20-msec calculation time. Extremely long (250 msec) calculation and update times could be tolerated without stability problems.

Performance degradation of the exhaust nozzle control limited update time to 50 msec for a 3.23-msec calculation time, and to 20 msec when calculation time and update time were identical. A delayed response of the afterburner light-off detector and exhaust nozzle overshoot with resulting fan oversuppression were the limiting factors. Extension of the update interval to 150 msec caused failure of the control due to a false indication by the blowout detector.

Two methods of implementing the complex exhaust nozzle control are given, one of which is designed to reduce sampling interval requirements and allow a more lengthy calculation time. In addition a modification of the exhaust nozzle control to provide for either velocity or position servoactuation systems is discussed.

INTRODUCTION

Interest in digital control systems for airbreathing aircraft is increasing. New objectives of quieter engines, shorter takeoff and landing capabilities, higher efficiencies with decreased mission costs and increased engine life cycles are placing higher demands on the control systems used. A close interaction of the airframe, inlet, and engine controls is becoming necessary, and the use of a digital computer in these flight systems is desirable as an efficient means of achieving this interaction.

A starting point for a program utilizing the capabilities of digital control to exercise improved control modes can be a basic digital program that reproduces the functions of the standard bill-of-materials (BOM) control modes for an engine. This computer program must permit efficient utilization of the digital computer's core capacity and computing time so computing capacity is left for extended capabilities such as integrating inlet and engine controls, self-optimizing controls, and so forth. The basic BOM computer program must also provide control accuracy and dynamics comparable to the hydromechanical system using only sampled information.

The purpose of this report is to document a digital computer program which satisfies the previous objectives for the TF30-P-3 turbofan engine. This control duplicates the function of the existing hydromechanical control, using control laws and logic paralleling that used by the hydromechanical control. The techniques used are sufficiently general that they may be used to produce digital versions of other, similar controls with a minimum amount of effort.

A description of the TF30-P-3 hydromechanical control is presented first. The digital problems of function generation and stability of internal dynamic loops are then considered as they apply to the TF30-P-3 control. A digital implementation of the control using a process control computer follows. This control is then used in conjuction with a real time simulation of the TF30-P-3 engine to evaluate the operating characteristics of the finite state controller. Data obtained from the simulation is presented to illustrate the effects of calculation and update times and to compare the different exhaust nozzle programming schemes.

DESCRIPTION OF THE TF30-P-3 ENGINE AND CONTROL

The TF30-P-3 is a twin-spool turbofan engine equipped with an afterburner. The engine, shown schematically in figure 1, includes a three-stage axial-flow fan mounted on the same shaft with a six-stage axial-flow low-pressure compressor. This unit is driven by a three-stage low-pressure turbine. A seven-stage axial-flow compressor driven by a single-stage air-cooled turbine makes up the high-pressure spool.

The engine has a hydraulically actuated variable exhaust nozzle and seventh-stage (low-pressure) and twelfth-stage (high-pressure) compressor bleeds. The afterburner consists of a diffuser duct, a combustion chamber, a flameholder, and seven fuel spray rings arranged so as to identify five separate afterburning zones.

Main Fuel Control

A block diagram of the main fuel control is given in figure 2. To help the reader, the diagram is divided into three distinct areas separated by the dot-dash lines. All symbols used are defined in appendix A. The upper left portion of the diagram is the speed request calculation area. A desired high rotor speed Npt is developed as a function (MFC2) of power lever angle PLA, inlet total temperature $Tt2$ and pressure $Pt2$ (functions MFC3 and MFC4). When the power lever reaches the afterburner request point of 70°, Npt becomes a function of $Tt2$ and $Pt2$ only. The desired speed Npt is upper and lower limited by the maximum and minimum speed schedules according to inlet total temperature and Mach number MN to form the requested speed $NREQ$. The maximum speed is increased somewhat by removal of the signal through KN, if afterburning is requested.

The center portion of the diagram exhibits the acceleration and speed governor controls. Actual speed $N2$ is subtracted from $NREQ$, multiplied by a proportional gain Kg, and biased by the governor breakpoint fuel flow to burner pressure ratio Wf/Pb to form the proportional control's desired Wf/Pb ratio $POBL$. This ratio is upper limited during acceleration and lower limited during deceleration to form the WFPB signal. The acceleration schedule MFC1 is a function of $Tt2$ and $N2$ and is designed to avoid turbine overtemperature and compressor stall, while the deceleration schedule is simply the constant Wf/Pb. A signal $TL6$ is generated for the ex-

3

haust nozzle control to indicate when WFPB is at least 9.87×10^{-4} $(kg/hr)/(N/m^2)$ less than the acceleration schedule limit.

The actual calculation of fuel flow is illustrated in the right-hand portion of figure 2. The WFPB command is multiplied by burner pressure Pb to determine a fuel flow. Changes in this flow are rate limited, and the magnitude of the flow is both upper and lower limited. If no afterburner blowout signal (TL5 = 0) is received from the afterburner control and no engine shutdown is requested by a power lever position below 10°, this calculated flow becomes commanded fuel flow Wfc. During a detected afterburner blowout (TL5 = 1), the desired Wf/Pb ratio is determined as a function of burner pressure by a blowout derichment schedule MFC7 and becomes independent of speed. This modified ratio (WFBO) is multiplied by burner pressure and the control switches over to the resulting fuel flow command until TL5 is reset to zero. The TL5 signal may be reset by the exhaust nozzle area dropping below an area corresponding to 24° rotation of the exhaust nozzle pulley actuator, or a decrease in speed below the afterburner turnon point (see fig. 3).

Exhaust Nozzle Control

A block diagram of the exhaust nozzle control is presented in figure 3. The diagram is divided by the dot-dash lines into four distinct areas for easy reference.

The basic function of the exhaust nozzle control is to maintain a desired burner pressure to turbine exit pressure ratio $(Pb/Pt7)_s$ during afterburner operation. The Pb/Pt7 schedule is a function of high rotor speed and burner pressure (ENC1 of fig. 2 and the Pb/Pt7 bias schedule) and will be called supression ratio Pb/Pt7 for reference. In addition the control performs afterburner light-off and blowout detection, and provides a command to the afterburner fuel control.

Logic to ensure proper sequencing and timing of the afterburner is also provided by the exhaust nozzle control (center portion, fig. 3). Prior to light-off, the blowout and light-off detectors, TL3 and TP2, the B/O & F/C relay valve lock, and the B/O & F/C relay valve are zero. When PLA is advanced beyond 70°, TL1 energizes the P/L shuttle valve. When the engine reaches speed, a PR3 turn on signal is received from the main fuel control. This signal will pass to the light-off detector and afterburner fuel control as T05 provided the engine is off the acceleration schedule by a small amount (TL6 = 1). Once T05 has become energized, the

4

acceleration requirement is eliminated by the PXG relay valve operation. As soon as T05 becomes 1, a small positive value (ERX) is passed to the zone fuel flow command piston (XOO). This is illustrated in the right-hand portion of figure 3. The ERX signal is integrated by the XOO piston to a small value determined by the Wf/Pb cam rise feedback schedule ENC6 and the commanded value XRQ from the correlation cam (ENC5). This XOO position determines the initial light-off fuel flow. At the same time, IA14 goes high, arming the light-off detector (TP2, center of diagram) to trip as soon as PPE increases 3 percent (L/O release schedule) above any minimum it may achieve before light off. The light-off detector will remain tripped as long as T05 remains high.

When lightoff is detected (TP2 = 1), the exhaust nozzle control is essentially a position servo with a proportional plus integral control on suppression ratio error PPE in the feedback path (lower left portion of fig. 3). The tripping of TP2 allows the integrator in the proportional plus integral control to integrate from its zero initial position and the loop around the exhaust nozzle actuator is closed, freeing the actuator from the hard closed command velocity which it had prior to lightoff. The output of the proportional plus integral control PIOT is a function of PPE, where PPE is calculated from the following equation:

$$PPE = function \ \ ENC2 \ (B7E)$$

where

$$B7E = K1 \left[1 - \frac{(Pb/Pt7)_m}{(Pb/Pt7)_s} \right]$$

and K1 is a unity gain constant which decreases when B7E exceeds 15 percent.

The commanded position into the feedback loop ARQ is either a function of power lever angle PLA, or an allowed position XAL derived from the zone fuel flow command XOO, whichever is smaller.

The exhaust nozzle position feedback AJP and the output from the proportional plus integral control PIOT are combined in the correlation cam ENC5. This cam essentially adds AJP and PIOT through variable, positive, or negative gains, and is used to produce the feedback to the actuator loop AFBX and to generate a command XRQ to the zone fuel control piston XOO. The primary function of this cam is to ensure that the opening of the exhaust nozzle will lead increases in commanded after-

burner fuel flow. By generating a negative command to the XOO piston, this cam has the ability to cut back on afterburner fuel flow should PIOT become excessive.

Whenever PPE drops below -15 percent, a blowout detection is possible. The blowout detector (left center portion of fig. 3) is armed by the exhaust nozzle opening 24° (TL4 = 1), and the PR3 turnon command which powers T05. Therefore, a blowout may not be detected unless a lightoff was previously detected. All these conditions being met, TL3 will go high, flip the B/O & F/C relay valve to turn off T05 and thereby reset the control for the next light-off detection. Note that if PLA is still advanced beyond 70°, the B/O & F/C relay valve lock will prevent the B/O & F/C relay valve from resetting, thus inhibiting future lightoffs until PLA drops below 68°. The blowout signal is delayed 0.1 second and then passed to the main fuel control as TL5.

In addition, a pop-open exhaust nozzle feature is provided for rapid thrust reduction when landing (upper left portion of fig. 3). It is activated by a squat switch, which detects when the plane is on the ground, and a power lever angle of less than 22°.

Afterburner Fuel Control

As seen from figure 4, afterburner fuel to burner pressure Wf/Pb ratios are scheduled for each zone as a function of the zone fuel flow command piston XOO. In addition, each zone's fuel flow is set to zero unless XOO passes the zone cutoff point.

Slightly beyond the cutoff point for zones 2 to 5 there is a hold position on the XOO piston (see lower right portion of fig. 3). As soon as this hold position is reached, the TVL limit timer is activated to hold XOO at this position. A description of the TVL limit timer operation is given in appendix B. This holding provides time for fuel to fill the zone fuel line. The amount of hold time is a function of burner pressure. If this hold timer were not implemented, the exhaust nozzle control would allow too rapid an increase in afterburner fuel flow since it would not "see" the large suppression ratio error caused by individual zone light-off transients until the deadtime needed to fill the fuel lines had elapsed. This additional phase lag in the loop would cause unstable operation; but after the line is filled, this phase lag no longer exists.

The shape of the Wf/Pb piston feedback cam (ENC6 on fig. 3) is designed to

6

provide hysteresis in the XOO piston loop so that sharp decreases in XRQ due to light-off transients will not cause XOO to pull back. Also note that the Wf/Pb piston velocity curve (ABC8) is such so as to allow XOO to integrate rapidly in the forward direction, but much more slowly in the reverse direction.

Bleed Door Control

The seventh-stage bleed is controlled by inlet Mach number and is closed for Mach numbers below 1.7 (see fig. 5). The twelfth-stage bleed operates on low compressor pressure ratio as follows: If the bleed is open, it will close when $Ps3 > K1_{bleed} \cdot Pt2 + K2_{bleed}$ and $dPs3/dt > 0.0$, where $Ps3$ is the low compressor static discharge pressure and $K1_{bleed}$ and $K2_{bleed}$ are constants. If the bleed is closed, it will open when $Ps3 \leq K3_{bleed} \cdot Pt2 + K4_{bleed}$ and $dPs3/dt \leq 0.0$, where $K3_{bleed}$ and $K4_{bleed}$ are constants greater than $K1_{bleed}$ and $K2_{bleed}$, respectively. The bleed will also open during a throttle chop (POBL < 12) or during an afterburner blowout (TL5 = 1).

CONSIDERATIONS IN DIGITAL CONTROL

Function Generation

One of the important aspects in building a control is the ability to generate the functions required. Functions of a single variable are easily generated by either linear interpolation between stored data points or by solving equations previously found by curve fitting the function.

Functions of two or more variables are not so easily handled, however. One cannot assume that acceptable results may be obtained by simply keeping one variable constant and generating two functions of the second variable to use in linear interpolation to obtain the desired result. Linear interpolation may be useless if the two single variable functions intersect or the first partial derivatives are discontinuous or contain points near infinity.

An example of interpolation difficulty is depicted by the small portion of the acceleration schedule reproduced in figure 6. Here, discontinuous first partial derivatives are illustrated by the sharp breakpoints, and the single variable functions in-

tersect. By interpolating along lines parallel to the axes and between two functions of high rotor speed at constant T_{t2}, a third function representing a constant T_{t2} between the original two functions is obtained (dashed line). Severe departure from the desired function occurs, partially because of the discontinuous partial derivatives, but mainly because linear interpolation forces all functions of constant T_{t2} between the original stored functions to intersect at the same point. For some functions, the errors introduced at the points of discontinuity or at a point where the partials are near infinity may be reduced by changing the interpolation axes or performing a linear transformation such as a change to corrected parameters. Reference 6 offers one such solution. These techniques, however, will not correct errors introduced because of the intersection of the single variable functions. The solution to such problems can become quite cumbersome and time consuming, and may require the introduction of additional functions or variables.

Fortunately the troublesome intervals which occur in the TF30-P-3 control either lie in a location where severe errors may be tolerated, or the errors which do result are so small as to be within acceptable limits. In the case of the acceleration schedule, the troublesome areas occur at speeds below idle and, therefore, will only affect engine startup. In addition, the errors are such so as to produce a more conservative acceleration schedule. The result is that the only detrimental effect of using linear interpolation is a slight increase in startup time. The other schedules which produce similar difficulties can also be tolerated as producing either acceptable, or negligible discrepancies. These schedules are the maximum speed limit MFC5 schedule, and the nonafterburning and afterburning biased speed request schedules of MFC3 and MFC4.

Internal Dynamic Loops

A second class of problems arising in digital control are those due to sampling, or to the discrete nature of the digital computer. Generally engine dynamics are slow enough such that control loops involving engine parameters are essentially unaffected by the digital computer's sampling limitations. Problems may arise if the control has self-contained fast response elements or control loops. Two such loops are identifiable within the TF30-P-3 hydromechanical afterburner control.

Figure 7 depicts the result obtained when the afterburner control is linearized

8

and simplified using maximum gains for the nonlinear elements and logic states which produce worst case internal loop conditions. In this case the maximum values of functions ENC5, ENC6, ENC7, and ABC8 are defined as:

$$\max \text{ENC5 (AJP)} = \text{Kac}$$
$$\max \text{ENC5 (PIOT)} = \text{Kpc}$$
$$\max \text{ENC6 (XOO)} = \text{Kc}$$
$$\max \text{ENC7 (SVX)} = \text{Kav}$$
$$\max \text{ABC8 (ERX)} = \text{Kpv}$$

In creating this one-for-one digital model of the hydromechanical control, a sampler is required to "break up" any loop whose output depends upon either externally sampled or previously calculated values. Although samplers may be placed in many positions to accomplish the required result, analysis and calculation is simplified if a minimum number of samplers are chosen. For the case in point, placing a sampler after the feedback loop summing junction for loops A and B is sufficient.

Zero-order holds are used on all analog outputs, and a deadtime of one sample interval is included wherever a value calculated during a previous update interval is used.

Assuming the loops involving engine dynamics will remain stable under sampling, there are two identifiable loops which must be investigated for stable operation. These loops are labeled as A and B in figure 7.

The stability of loops A and B can be investigated as follows. Referring to the variables as labeled in figure 7, the value of CR in the nth time interval was computed as

$$CR\ (n) = \left[XRQ\ (n) - 1.01\ CR\ (n - 1) \right] Kpv \cdot Kc \cdot T + CR\ (n - 1) \tag{1}$$

where T is the update time in seconds. Using z-transform theory, equation (1) can be converted to the following z-transform:

$$CR\ (z) = Kpv \cdot Kc \cdot T \cdot XRQ\ (z) + (1 - 1.01\ Kpv \cdot Kc \cdot T) \cdot [CR\ (z) \cdot z^{-1}]$$

or

$$\frac{CR\ (z)}{XRQ\ (z)} = \frac{Kpv \cdot Kc \cdot T \cdot z}{z + 1.01\ Kpv \cdot Kc \cdot T - 1} \tag{2}$$

9

For stability the root of the denominator of equation (2) must fall inside the unit circle. The root is given by

$$z = 1 - 1.01 \, Kpv \cdot Kc \cdot T$$

Hence, for stability

$$-1 < 1 - 1.01 \, Kpv \cdot Kc \cdot T < 1$$

Substituting the values of Kpv and Kc yields the result that loop A will be stable if $0 < T < 6.1$ msec.

For loop B analysis, the following relation (ref. 1) is used:

$$\frac{AFBX \, (z)}{ARQ \, (z)} = \frac{G \, (z)}{1 + G \, (z)}$$

where G(z) is the z-transform of the network between SVX and AFBX. In evaluating G(z) a calculation deadtime must be added to account for the fact that the output does not occur immediately after sampling. Note that no deadtime was needed for the loop A calculation since no input or output was involved. Assuming a calculation time equal to the update interval results in

$$\frac{AJP \, (z)}{ARQ \, (z)} = \frac{\dfrac{2.2 \, Kav \cdot Ks \cdot Kac \cdot T}{z \, (z - 1)}}{1 + \dfrac{2.2 \, Kav \cdot Ks \cdot Kac \cdot T}{z \, (z - 1)}} \tag{3}$$

Substituting the values of Kav, Ks, and Kac into equation (3) yields

$$\frac{AJP \, (z)}{ARQ \, (z)} = \frac{18T}{z^2 - z + 18T} \tag{4}$$

The roots of the denominator of equation (4) are given by

$$z = \frac{1}{2} \pm \sqrt{\frac{1}{4} - 18T}$$

Restricting the roots to lie within the unit circle for $T > 0$ results in

$$0 < T < 55.5 \text{ msec}$$

10

The previous results indicate that update times greater than 6.1 msec may produce control instability. This limitation is severe and unnecessary. It should be pointed out that the problem has arisen because of the closed loop nature of the hydromechanical design. It is possible to avoid loops A and B by implementing a feedforward equivalent of the control such as was done in reference 7. However, it is not necessary to involve the complication of a redesign. One need only iterate around loop A a sufficient number of times to ensure stability. A sufficient number of times is simply some integer m such that $T/m \leq 6.1$ msec. The procedure is to filter XRQ to produce m inputs to the loop for each update interval. For this control, a sample-and-hold filter was used. The m inputs thus produced were then used to calculate the loop as if it were operating at an update time of T/m seconds. Since the use of a sample-and-hold filter yields perfect knowledge of the current and future $m - 1$ inputs to the loop, the additional phase shift introduced by the filter can be effectively eliminated by advancing the iteration. For example, consider what happens if the current sampled value is held and put into the loop m times. The final result will be the same as if the update interval were T/m seconds, and the input assumed and held at the current value $T(m - 1)/m$ seconds earlier. This advance will more than cancel the phase lag generated by the sample-and-hold filter if $m > 2$. The additional phase lead helps minimize the phase lag produced by the sample-and-holds on the outputs.

By using this iterative technique, one obtains an approximation to an advanced z-transform (ref 3.) of the loop involved; but unlike an advanced z-transform, the technique is applicable to nonlinear systems. The approximation becomes better as m is increased. This subinterval type of iteration is preferable to iteration techniques such as Newton-Raphson in that the calculation time is limited to a fixed number of iterations. In Newton-Raphson, the error may not reduce to an acceptable level in the allotted number of iterations, causing unpredictable results. Through the use of subinterval iteration, then, internal dynamic loops need never restrict update times.

DIGITAL IMPLEMENTATION OF THE TF30-P-3 CONTROL

The techniques outlined previously were applied to implement the control from the block diagrams presented in figures 2 to 5. The procedure is straightforward,

and a one-to-one correspondence exists between the hydromechanical and digital control modes. A description of the TVL limit timer implementation is given in appendix B, and a flow chart of the exhaust nozzle calculation (ENC subroutine) is given in appendix C. A detailed flow chart of the entire program is available from the author on request.

To verify the digital implementation and to determine the effects of sampling, the control was programmed on a process control computer and used to run a real-time hybrid simulation of the engine. The configuration used is shown in figure 8. Free stream pressure, temperature, and Mach number were entered into the simulation to set the operating condition. Mach number and update time were entered into the digital control from a teletype during program initialization. A complete description of the hybrid engine simulation is given in reference 2.

Signals were received from the engine simulation as analog voltages. The control outputs, in the form of analog voltages, were entered into an analog simulation of the control fuel lines and actuators. The actuator simulation is shown in figure 9, and details of the digital computer are given in table I. The signal processing unit consists of buffer amplifers, readout devices, and patch boards used for convenience. For the digital computer, approximately 4800 of the read/write memory cells were needed, and only one of the two multiplexer, sample-and-hold, digitizer units were used, limiting the maximum sample rate to 20 000 samples per second. Table II lists the various parts of the program, their approximate memory requirements and calculation time.

An initialization program calculates the update time dependent constants used in the program. This initialization procedure is executed only once, and the constants calculated are stored as fixed values. An interval timer is used to issue an interrupt to the computer at a fixed rate equal to the specified update time. After receiving the interrupt, the computer begins sampling the input variables via a direct memory access controller. The computer then idles for approximately 400 microseconds waiting for an interrupt from the direct memory access controller indicating that all variables have been digitized and stored. After receiving this second interrupt, control calculation is begun. As indicated in table II, approximately 3.23 msec are needed to complete the calculation, leaving an additional idle period between the end of the control calculation and the next timer interrupt. During idle periods, the computer is available to display program variables to the operator. A timing diagram of the process is given in figure 10.

12

OPERATING CHARACTERISTICS

The control update interval determines how often the engine variables are sampled and how often the commands are updated. The control calculation time determines how much deadtime occurs between the sampling of the variables and the updating of the commands. Provided all internal dynamic loop problems have been properly handled, the maximum possible update intervals and calculation times will be determined by engine transient response. Since the engine is nonlinear, it would not suffice to evaluate these maximums at a single operating point. For this reason, throttle bursts from idle to intermediate and from intermediate to maximum were used for evaluation purposes. All results were taken at sea-level static conditions. Unless indicated otherwise, a control calculation time of 3.23 msec was used.

Main Fuel Control

Figure 11 shows some important engine parameters during a throttle burst from idle to intermediate. Total mass flow is included as an indicator of engine thrust, since thrust itself was not available from the simulation. Inspection of the figure indicates that all parameters stay well within safe operating limits for update times as great as 249 msec. Update times beyond 249 msec could not be investigated, as this was the maximum time permitted by the scaling of the update time dependent parameters.

The important observation is that no significant performance change could be detected in the engine variables for update times to 75 msec. For the two rotor speeds, the response was nearly identical for update times to 150 msec. Such a broad range of operation indicates that digitizing the control has had negligible effect on its response to power lever commands. In addition, the major penalty for extremely long update times is an increased control response time. A verification of this fact can be seen from the high pressure compressor ratio response, shown in figure 12. It is seen that stall margin improves as update time is increased. Although there is some ambiguity as to the exact location of the stall line, more than adequate stall margin exists for all operating conditions.

Performance changes due to increasing update time show up best in the high pressure compressor ratio response. Observation of this response indicates a small

(2 percent or less) increase in stall margin for update times between 50 and 75 msec, this difference was too small to be conveniently included in figure 12. With the increased sensitivity of this map, there is still no evidence of any benefit to updating faster than every 50 msec.

Increasing the physical time it takes the computer to perform the control calculation will introduce an additional deadtime into the control loop. This pure phase lag will have an effect on transient response in addition to those produced by increased update times. The response shown in figure 13 illustrates the point. Two responses to a throttle burst from idle to intermediate for a 150-msec update interval are compared to the 3.5-msec update, 3.23-msec calculation time response. The difference between the two responses occurs in the amount of delay introduced by the calculation time. It is observed that the additional delay imposed by a 150-msec calculation time is greater than that delay produced by a 150-msec update interval alone. In general, this statement will be true since the phase lag of a sample-and-hold is equivalent to a deadtime of only half an update interval. The effect of making calculation time equal to update time is illustrated in figure 14. For this case, performance degradation occurs at update intervals greater than 20 msec.

Noniterative Exhaust Nozzle Control

Since the linearized analysis of the internal dynamic loops of the exhaust nozzle control assumed worst case conditions, a test of a noniterative exhaust nozzle control was performed to determine where the practical limits would lie. Figures 15, 16, and 17 illustrate the results. The control is seen to operate properly for a 3.5-msec update interval (fig. 15); but at a 10-msec interval (fig. 16), loop A begins to oscillate. This is in reasonable agreement with the predicted value of 6.1 msec. The effect of the oscillation is seen in the commanded afterburner fuel flow. At times this flow is proportional to XOO, and it is at these times that a loop A oscillation is reflected in zone fuel flow. At an update time of 40 msec (fig. 17), the oscillation becomes so severe that it overides the PLA input command to the exhaust nozzle loop (loop B), causing the nozzle to jitter.

14

Iterative Exhaust Nozzle Control

The subinterval type of iteration as previously described was performed around loop A of the exhaust nozzle control to produce what will be referred to as the iterative exhaust nozzle control. It is this version which is represented by the exhaust nozzle control (ENC subroutine) flow chart in appendix C. An iteration time of 5 msec was used. From the data to be presented, this time is seen to be sufficiently fast to obtain an acceptable approximation to the desired control.

A throttle transient from intermediate to maximum is shown in figure 18. At a 50-msec update interval, performance of this control is still quite acceptable. The 25-msec earlier start of zone 1 fuel flow is due to the calculation advance produced by the iteration around loop A. The advance is generated on the switching of T05 in a similar fashion as the advance which occurs on the XRQ input. This advance calculates to 45 msec, but only 25 msec is seen because of a potential lag of 50 msec on the sampling of throttle position demanding afterburner operation. The advance is desirable to offset this delay on PLA. The 25-msec early rise in exhaust nozzle position occurs because of an early light off due to the early fuel flow.

The early light off of the remaining afterburner zones is partially due to phase lead generated by the iterative loop and partially due to the rounding which occurs when determining the required TVL limit timer hold time. The hold time must be an integer subdivision of the update time and is rounded down if the remainder is less than half of an update interval.

Figure 19 gives a more complete set of engine parameters for a throttle burst from intermediate to maximum. At the 120-msec update time presented, there are several notable occurrences. First, there is no evidence of loop B becoming unstable, even though the predicted maximum of 55 msec for a noniterative calculation has been exceeded. This discrepancy might be expected because of the fact that the actuator is held to its maximum slew limit during most of the transient, thus greatly reducing loop gain. A second consideration is that the calculation time is shorter than the assumed worst case value of one update interval. Zero calculation time in dicates instability wouldn't occur until a 111-msec update interval was reached. The second feature of the response is that the exhaust nozzle starts opening late, even though zone 1 fuel flow begins early. This indicates the occurrence of a delayed light-off detection. Since the control is inhibited during the period between zone 1

turn on and light-off detection, the turn on of the remaining zones begins late. Likewise, this delay has added to the phase delays produced by the longer update interval, aggravating an overshoot of exhaust nozzle position during the first 2 seconds of the transient.

Light-off detection proves to be the ultimate restriction on update time. Figure 20 illustrates what happens when update times of 150 msec are attempted. Because of the phase shift added by the delay and a nearly unstable loop B, the control becomes unstable in the time shortly following light-off. The sequence of events is as follows. Excessive overshoot of the nozzle causes severe oversupression. This oversupression causes an excessively negative supression ratio error such that the blowout detector is tripped. Once the blowout detector trips, the control turns off the afterburner and switches the main fuel calculation to the blowout derichment schedule. The rapid turnoff of the afterburner with the nozzle being open causes main burner pressure to drop. Fuel flow thus drops, with the process continuing until the exhaust nozzle closes sufficiently to reset the blowout detector. The normal fuel control then slowly brings the engine back to the prelight-off operating point.

A practical limit on update time for the exhaust nozzle control is therefore defined as that point at which nozzle overshoot and oversupression become excessive. Practically, this point is around 50 msec.

As was done for the main fuel control, the effects of increased calculation time on the afterburner control must also be considered. Figure 21 depicts these effects. The calculation advance produced by the iteration of loop A is cancelled by the delays of the increased calculation time. In addition, the assumed worst case calculation time of one update interval used to determine the maximum allowable update time of 55 msec is now more accurate. Zone light offs are now increasingly delayed as the update and calculation times are increased. Acceptable operation can now only be obtained for a 20-msec update interval. If the iterative loop were to be replaced by a feed-forward type of implementation, phase lead such as that obtained by using an advanced z-transform, would have to be added in order to obtain proper operation at update times comparable to those of the main fuel control.

Modified Iterative Exhaust Nozzle Control

For failsafe reasons, it may be desirable to operate the exhaust nozzle with an

external position type of actuation system. To demonstrate that the control can easily accommodate such a system, the configuration of figure 22 was tested. In order to compensate for the inherent first-order lag produced by the position servo, a proportional plus integral control with AJV as its input was added. The net result to the control loop is a near return to the simple integration of AJV to produce position. To compare the two systems, refer to figure 7.

Since the actuator velocity limits were used to limit the AJV command, the integrator on AJV from the proportional plus integral control should be an accurate indication of exhaust nozzle position. Hence, two versions of the control were tried, one using actual position as the feedback, and one using the predicted position as the feedback. Note that the second system is a feed-forward control of the exhaust nozzle actuator. The performance of these two systems for a 50-msec update interval is seen in figures 23 and 24. The lead on zone 1 turn on is due to causes similar to those of figure 18. The response of this control is nearly identical to that of the conventional iterative control and has acceptable performance at a 50-msec update interval. Figure 24 indicates that the predicted exhaust nozzle position is an accurate estimate of the actual position, and that the performance of the control using this predicted value is also acceptable for a 50-msec update interval.

The exhaust nozzle position servo actuation system has definite advantages. The accuracy of the predicted position provides a signal to compare with the measured position to determine if the actuator is functioning properly. This signal, along with the suppression ratio error, can then be used to effect a fail operational system. If both suppression ratio and the predicted versus actual position errors become large, the indication is that the exhaust nozzle is malfunctioning. A limitation against afterburner operation should then be imposed. However, if only the position error is excessive, the indication is that only the position feedback transducer path is malfunctioning and feed-forward operation can then be employed for a restrictionless afterburner operation. The aforementioned fail operational system was not implemented but is offered as an indication of the versatility of the digital computer and the advantages of employing a redundant electrical system.

CONCLUDING REMARKS

A digital control can easily duplicate standard hydromechanical turbojet control

functions. If fast response internal dynamic loops are required within the control, the problem of instability can be avoided by using an iteration technique which effectively subdivides the update time into smaller increments. In addition, a method is available to determine the maximum update interval which ensures stability of these loops.

A digital control similar in operation to the standard bill-of-materials control for the TF30-P-3 engine was proven feasible by having a process control computer implementation successfully control a real time simulation of the engine. The program required approximately 4800 words of storage and 3.23 msec for calculation. Using the programming techniques presented, calculation times up to 20 msec had negligible effect on control operation and, for 3.23-msec calculation times, update times as large as 75 msec for the main fuel and 50 msec for the exhaust nozzle control could be tolerated before performance degradation took place. Sufficient computing capability is therefore available for increased control complexity such as including integrated or self-optimizing, self-correcting control schemes.

Lewis Research Center,
National Aeronautics and Space Administration,
Cleveland, Ohio, October 7, 1974,
501-24.

APPENDIX A

SYMBOLS

ABC1 – ABC5	afterburning fuel flow ratio schedule for zones 1 to 5, kg/hr
ABC6	Pb bias schedule
ABC8	Wf/Pb piston velocity schedule
ACR	correlation cam output function of AJP and PIOT
AFBX	feedback from correlation cam to exhaust nozzle actuator loop
AJ	exhaust nozzle area, cm^2
AJP	exhaust nozzle feedback pully position, deg
AJPC	exhaust nozzle feedback pully position command, deg
AJV	velocity command to exhaust nozzle actuator, deg pully rotation/ sec
ARM	light-off detector track on supression ratio error
ARQ	commanded exhaust nozzle pully position, deg
A$OT	power lever drive to exhaust nozzle
BL7	low pressure compressor or seventh-stage bleed command
BL12	high pressure compressor or twelfth-stage bleed
B7E	supression ratio error
CATCH	TVL limit timer hold positions on XOO
CR	value of Wf/Pb feedback cam rise
d	denominator
ENC	subroutine which calculates exhaust nozzle control
ENC1	supression ratio schedule
ENC2	pressure ratio mixing cam characteristic
ENC3	proportional plus integral control integrator

ENC4	schedule of TVL limit timer hold time
ENC5	correlation cam schedule
ENC6	afterburner Wf/Pb feedback cam rise schedule
ENC7	exhaust nozzle actuator velocity schedule
ENC8	supression ratio bias schedule
ERX	error term in afterburner Wf/Pb piston loop
HOL	index for TVL limit timer
HOLDTIME	TVL limit timer hold time, sec
HOLT	number of update intervals in HOLDTIME
IA14	logic for light-off relay
IDLETRIM	addition to minimum speed schedule to trim for idle speed, rpm
IPVD	integral velocity in proportional plus integral control
Kac	maximum correlation cam gain to exhaust nozzle actuator position signal
Kav	maximum exhaust nozzle actuator velocity, deg/sec
Kb	integral gain of bleed door actuators, percent/sec
Kc	maximum gain of afterburner Wf/Pb feedback cam
Kg	governor gain, $(kg/hr)/[(N/m^2)(rpm)]$
KM	infinite gain
KN	maximum speed schedule bias, rpm
KPB	bias on supression ratio schedule as function of Pb
Kpc	maximum correlation cam gain to PIOT
Kpv	maximum afterburner Wf/Pb piston velocity
Ks	exhaust nozzle actuator integration rate, deg/sec
K1 - K6	constants
LOOP	number of iterations per update interval on exhaust nozzle control implicit loop

20

LOPC	counter for exhaust nozzle control implicit loop (equals LOOP at start of each update interval)
MFC1	acceleration schedule
MFC2	speed request schedule
MFC3	nonafterburning bias schedule for MFC2
MFC4	afterburning bias schedule for MFC2
MFC5	maximum speed schedule
MFC6	minimum speed schedule
MFC7	blowout derichment schedule over range of Mach numbers (i.e., function MFC6 reduced to function of Tt2 only)
MILTRIM	trim on power lever for intermediate speed
MN	Mach number
n	numerator
NREQ	speed request from power lever and schedules
Npt	desired high rotor speed, rpm
N1	low rotor speed, rpm
N2	high rotor speed, rpm
Pb	burner pressure, N/m^2
PBT	burner pressure biased to temperature
PIOT	output of proportional plus integral control
PLA	power lever angle, deg
PLAx	power lever command, deg
Po	free stream static pressure
POBL	main fuel control desired Wf/Pb units, $(kg/hr)/(N/m^2)$
PPE	modified supression ratio error
Ps3	static pressure, station 3

Pt2	total pressure at engine face
Pt7	turbine exit total pressure
S	Laplace variable
SPR	power lever speed request
SVX	exhaust nozzle actuator servovalve drive
T	update interval, sec
TC1 - TC3	fuel valve time constants
TL1	logic for power lever shuttle valve
TL2	logic of B/O & F/C relay valve lock
TL3	logic of B/O arm valve
TL5	blowout signal logic
TL6	PXG turn on logic
To	free stream total temperature
TO1	PR3 turn on logic
TO2	logic of power lever shuttle valve
TO3	logic of decel T/O arm valve
TO5	logic of PXG relay valve
TP2	logic of light-off detector
TSS	error in exhaust nozzle control loop
Tt2	compressor inlet total temperature, $^{\mathrm{O}}$C
TVLTIM	subroutine which determines TVL limit timer operation
T5	turbine inlet temperature, $^{\mathrm{O}}$C
Wf	main fuel flow, kg/hr
WFBO	blowout derichment schedule Wf/Pb units, $(\mathrm{kg/hr})/(\mathrm{N/m}^2)$
Wfc	commanded main fuel flow, кg/hr
WFPB	commanded main fuel to burner pressure units, $(\mathrm{kg/hr})/(\mathrm{N/m}^2)$

WFZ1 – WFZ5	afterburner fuel flow command for zones 1 to 5, kg/hr
WSPA	acceleration schedule Wf/Pb units, $(kg/hr)/(N/m^2)$
XAL	exhaust nozzle position allowed by zone fuel flow command position
XBL7	low pressure compressor bleed door position
XBL12	high pressure compressor bleed door position
XOO	afterburner Wf/Pb piston position
$\dot{XOO}$	first time derivitive of XOO
XOOL	last value of XOO
XOS	hold logic for TVL limit timer
XRQ	correlation cam drive to afterburner Wf/Pb piston
XWF	main fuel flow, kg/hr
XWFZ1 – XWFZ5	afterburner fuel flow for zones 1 to 5

Subscripts:

bleed	pertaining to the bleed door control
i	intermediate
m	measured
max	maximum
min	minimum
s	scheduled

APPENDIX B

DESCRIPTION OF TVL LIMIT TIMER

(TVLTIM SUBROUTINE)

The TVL limit timer temporarily limits the travel of the afterburner Wf/Pb piston (XOO) at four catch positions. The purpose is to allow time for afterburner fuel flow to fill the afterburner fuel lines. The number of update intervals that XOO is held is determined by the negative number in HOL, where

$$HOL = \frac{-HOLDTIME}{T}$$

Prior to the TVL limit timer operation, the ENC subroutine calculates XOO using the last output XOS of the TVL limit timer. This calculated value of XOO along with the last value of XOO (XOOL) is used by the timer routine in the following manner: The timer is started when

$$XOOL < CATCH \quad and \quad XOO \geq CATCH$$

The timer is reset when the timer times out or when

$$XOOL \geq CATCH \quad and \quad XOO < CATCH$$

To start the timer, XOO is placed on the catch to its hold position, HOLT is set equal to HOL and XOS is set equal to -1. To reset the timer, HOLT is cleared to -1 and XOS is cleared to zero. During normal timer operation, the interval timer counter HOLT is incremented when leaving the implicit loop calculation of the ENC subroutine. If HOLT then becomes zero, the indication is that the timer has timed out during the last update interval and the timer is reset as indicated previously. The flow chart for Subroutine TVLTIM is given on the following pages. The catch positions are listed numerically next to their respective comparator logic elements.

24

TVLTIM

I3$4

XOO

=0.7063   >0.7063

P

<0.7063

XOOL   =0.7063

<0.7063

XOO = 0.7063

TSET

>0.7063

XOOL   <0.9659

≥0.9659

RSET

XOO   ≥0.462

<0.462

=0.462   XOOL   <0.462

XOO = 0.462

TSET

>0.462

<0.252   XOO

B24

<0.7063   XOOL

≥0.7063

RSET

≥0.252

=0.252   XOOL   <0.252

>0.252

XOO = 0.252

TSET

<0.462   XOOL

≥0.462

RSET

B24
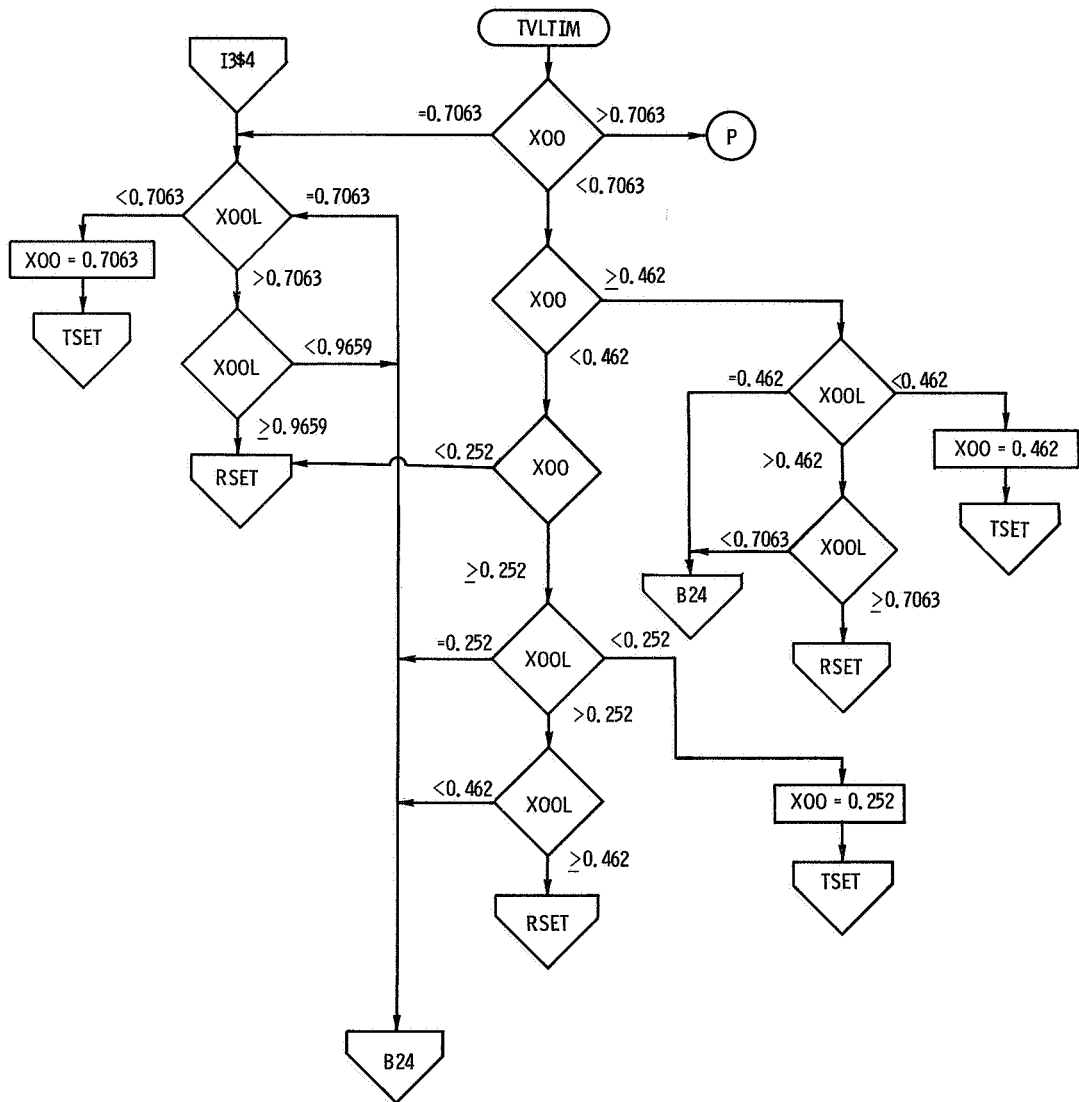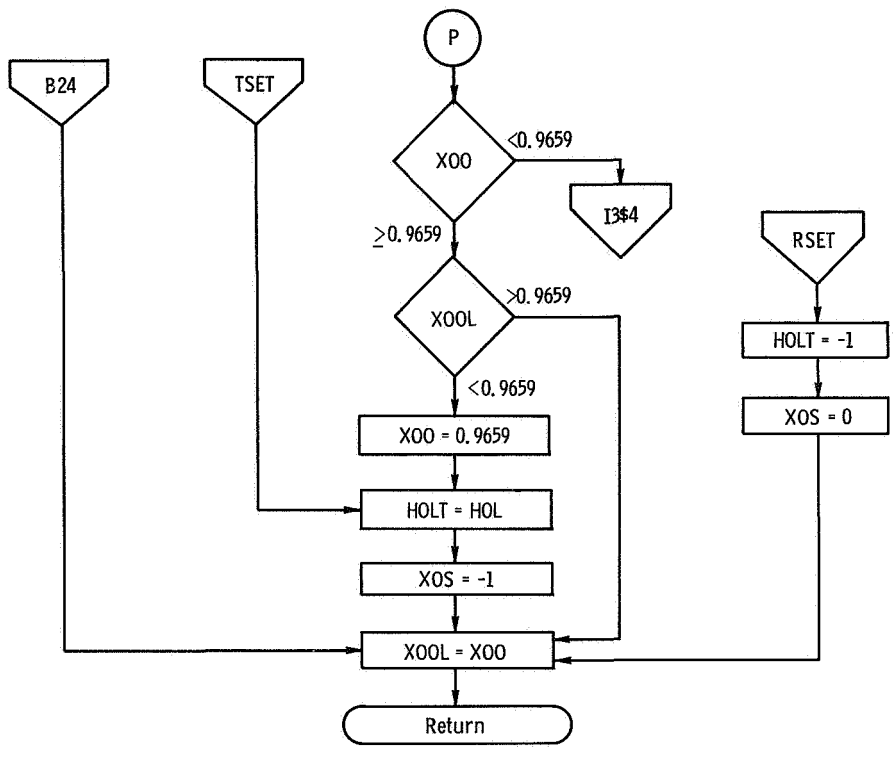
FLOW CHART (ITERATIVE VERSION) OF SUBROUTINE ENC

Iteration

ENC

Calculate correlation cam
AFBX = 2.2 f(PIOT,AJP)
(ENC5)

XRQ = AFBX

Limit AFBX
$AFBX_{min} \leq AFBX \leq AFBX_{max}$

Limit XRQ
$XRQ_{min} \leq XRQ \leq XRQ_{max}$

$XRQ = \frac{2.01}{2.2} XRQ$

ERX = XRQ - 1.01 CR

K

K

TO5

≥ 0

ERX = -0.01

< 0

XOS

< 0

≥ 0

ERX

≤ 0

> 0

ERX = 0

Limit ERX
$ERX_{min} \leq ERX \leq ERX_{max}$

Calculate afterburner
Wf/Pb piston velocity
XOO = f(ERX)
(ABC8)

XOS

≥ 0

< 0

$XOO = \frac{1}{6} \int \dot{XOO}$

$XOO = \int \dot{XOO}$

Limit XOO
$0 \leq XOO \leq 1.176$

L

27

L

Call TVLTIM

Calculate Wf/Pb
cam rise
CR = f(XOO)
(ENC6)

LOPC = LOPC - 1

LOPC
>0 → Iteration
=0

XAL = 0.345 CR + 0.0156

M

M

XAL
≤ A$OT
>A$OT

TSS = 3.2 XAL - AFBX

TSS = 3.2 A$OT - AFBX

Limit TSS
$TSS_{min} \leq TSS \leq TSS_{max}$

Squat
switch
On ground   Airborne

TP2
≥0
<0

TSS = -0.05

PLA
>22°   ≤22°

TSS = 0.019

Call actuator velocity
AJV = 43.7 f(TSS)
(ENC7)

N

N

HOLT = HOLT + 1

HOLT
<0
=0

HOLT = -1

XOS = 0

Return

28

REFERENCES

1. Tou, Julius T.: Digital and Sampled-Data Control Systems. McGraw-Hill Co., Inc., 1959.

2. Szuch, John R.; and Bruton, William M.: Real-Time Simulation of the TF30-P-3 Turbofan Engine Using a Hybrid Computer. NASA TM X-3106, 1974.

3. Saucedo, Roberto; and Schiring, Earl E.: Introduction to Continuous and Digital Control Systems. Macmillan Co., 1968.

4. Arpasi, Dale J.; Zeller, John R.; and Batterton, Peter G.: A General Purpose Digital System for On-Line Control of Airbreathing Propulsion Systems. NASA TM X-2168, 1971.

5. Kuo, Benjamin C.: Analysis and Synthesis of Sampled-Data Control Systems. Prentice-Hall, Inc., 1963.

6. Hart, Clint E.: Function Generation Subprograms for Use in Digital Simulations. NASA TM X-71526, 1974.

7. Batterton, Peter G.; Arpasi, Dale J.; and Baumbick, Robert J.: Digital Integrated Control of a Mach 2.5 Mixed-Compression Supersonic Inlet and Augmented Mixed-Flow Turbofan Engine. NASA TM X-3075, 1974.

TABLE I. - DIGITAL SYSTEM CAPABILITIES

Digital computer	
Magnetic core memory size, words	16 384
Word length, bits plus parity	16
Memory cycle time, nsec	750
Add time, μsec	1.5
Subtract time, μsec	1.5
Multiply time, μsec	4.5
Divide time, μsec	8.25
Load time, μsec	1.5
Store time, μsec	1.5
Indirect addressing	Infinite
Indexing	Total memory
Priority interrupts	28 Separate levels
Index registers:	
Independent	1
In conjunction with lower accumulator	1
Physical size, cm (in.)	
Width	61 (24)
Height	157 (62)
Depth	76 (30)
Interval timers	
Complement	2
Accuracy, clock pulses	±1
Clock rates, kHz	572, 286, 160, 143, 80, 71.5, 40, 35.75, 20, 10
Counter	16-Bit binary
Output	Priority interrupt to computer
Analog acquisition unit	
Number of multiplexers, digitizers, sample-and-holds	2
Overall sample rate (maximum), kHz	40
Resolution of digital data, bits	12 (plus sign)
Output code	Two's complement
Number of channels	64
Input range, V full scale	±10
Input impedance, MΩ (shunted by 10 pF)	10
Maximum source resistance, Ω	1000
Conversion time, μsec	38
Input setting time, μsec	9
Sample-and-hold aperture time, nsec	500
Safe input voltages, V	±20 sustained ±100 for less than 100 μsec
Total error with calibration, percent	0.073

TABLE I. – Concluded. DIGITAL SYSTEM CAPABILITIES

Frequency acquisition unit	
Number of channels	10
Nature of input	Continuously varying or pulsatile
Resolution of digital data, bits	12
Switch selectable clock rates, kHz	20, 80, 100, 400, external
Overall accuracy, bits	±1
Update rate	Once per cycle of input frequency
Maximum input frequency, kHz	1
Input amplitude range	100 mV to 30 V (peak to peak)
Analog output unit	
Total number of digital-to-analog conversion channels	26
Resolution (10 channels), bits	12 (plus sign)
Resolution (16 channels), bits	11 (plus sign)
Output voltage range, V full scale	±10
Output current (maximum), mA	10
Output impedance, Ω	<1
Accuracy (12 bit), percent of full scale	±0.1
Accuracy (13 bit), percent of full scale	±0.05
Slew rate, V/μsec	1
Settling time for 10-V step to within 0.05 percent of final value, μsec	20
Logical output unit	
Number of electronic switch outputs	32
Number of contact closure outputs	32
Maximum voltage, V	30
Maximum current, mA	100
Priority interrupt processor	
Number of channels	10
Input impedance, kΩ	47
Input voltage range, V	±10
Comparator switching	Trigger on rise or fall
Comparator hysteresis, mV	Adjustable from 35 to 650
Comparator output, V	+7
Monostable multivibrator:	
Pulse width, μsec	0.3
Pulse height, V	+7

TABLE II. - CONTROL MEMORY AND TIMING REQUIREMENTS

[Control calculation plus sample time, 3.23 msec.]

Routine name	Routine function	Memory words required	Memory cycles required		Computation time, msec[a]	
			Minimum	Maximum	Minimum	Maximum
FG	Single variable function generation	26	64	64	0.048	0.048
FG2D	Two variable function generation	79	133 + 2 FG	[b]149 + 2 FG	0.100 + 2 FG	0.112 + 2 FG
TIME	Timer and data acquisition control	13	22	22	0.017	0.017
EOB	Input scaling, calling of subroutines, and control outputs	272	236	246	0.177	0.185
SPREQ	Speed biasing and limiting for inlet conditions and afterburner operation	121	67 + FG + 2 FG2D	69 + FG + 2 FG2D	0.050	0.052
WFCOMP	Main fuel calculation and supression ratio scheduling	248	272 + 2 FG + 2 FG2D	316 + 4 FG + 2 FG2D	0.204	0.237
IPCTRL	Exhaust nozzle integral proportional control, light-off detector, afterburner zone 1 turn on	84	86	113 + FG	0.065	0.085
ENC	Correlation between afterburner fuel and exhaust nozzle	180	94 + FG + FG2D + TVLTIM	[b]121 + 2 FG + FG2D + TVLTIM	0.071	0.091
TVLTIM	TVL limit timer	68	21	40	0.016	0.030
BLEED	Bleed door control	56	51	61	0.038	0.046
AB	Afterburner fuel flow calculation	272	229	[b]825	0.172	0.619
MAIN	Program initialization	238	(c)	(c)	(c)	(c)
BLOCK DATA	Data for schedules	3176	(d)	(d)	(d)	(d)
Total control calculation		4833	2639	3774	1.98	2.83

[a]Based on memory cycle time of 750 nsec.
[b]Based on independent variable of function changing only one tabulated value per update interval (see text).
[c]Executed only once upon program start.
[d]Nonexecutable data.

High pressure
compressor
bleed

Customer
overboard
airbleed

Duct

Low pressure
compressor
bleed

Fan O. D.

Fan I. D.

Low pressure
compressor

Low
pressure
turbines

High
pressure
turbine

Burner

High
pressure
compressor

Inlet
diffuser
and duct

Engine stations   0   1   2   3   4   5   6   7   8   9
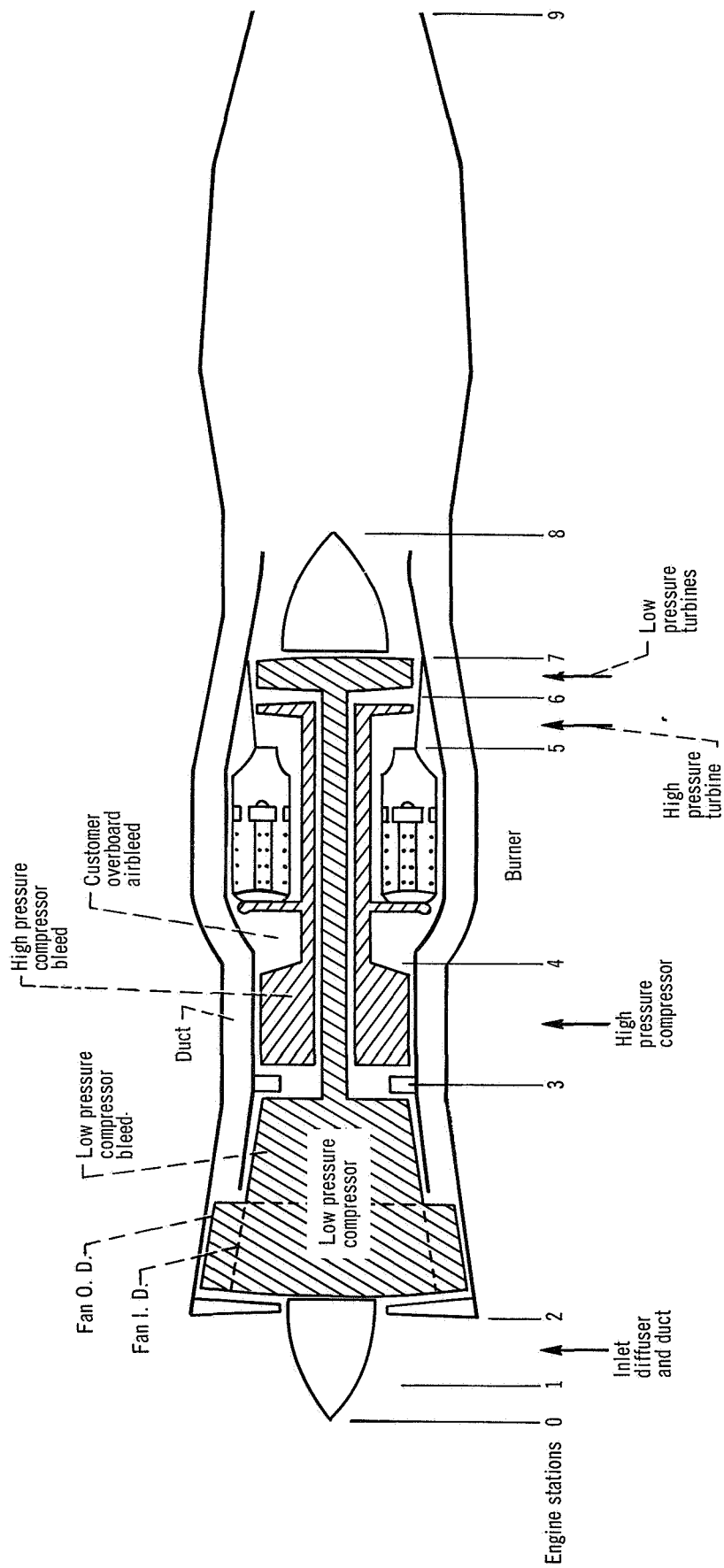
Figure 1. – Station identification.

33
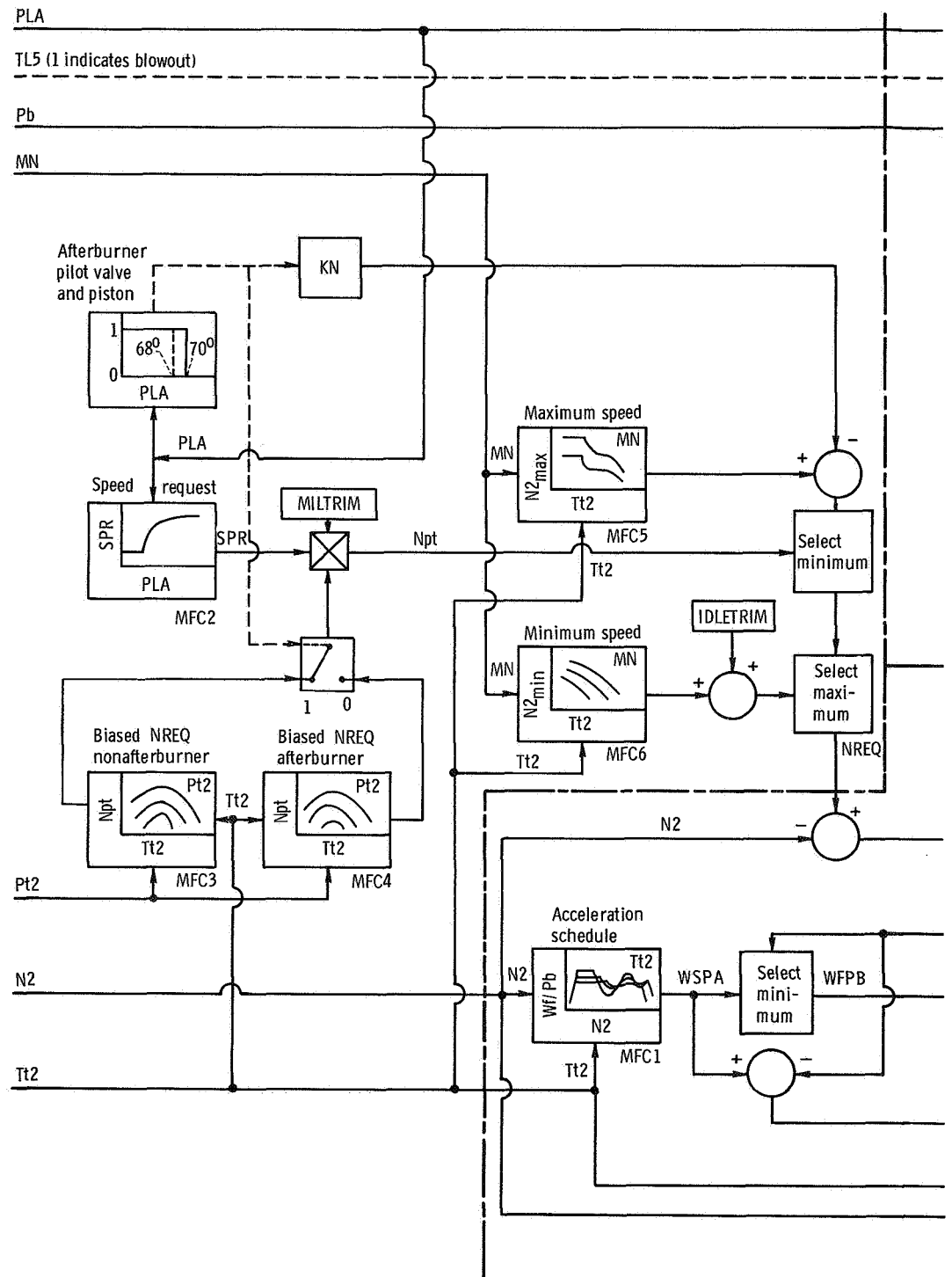
Figure 2. - Main fuel control

34
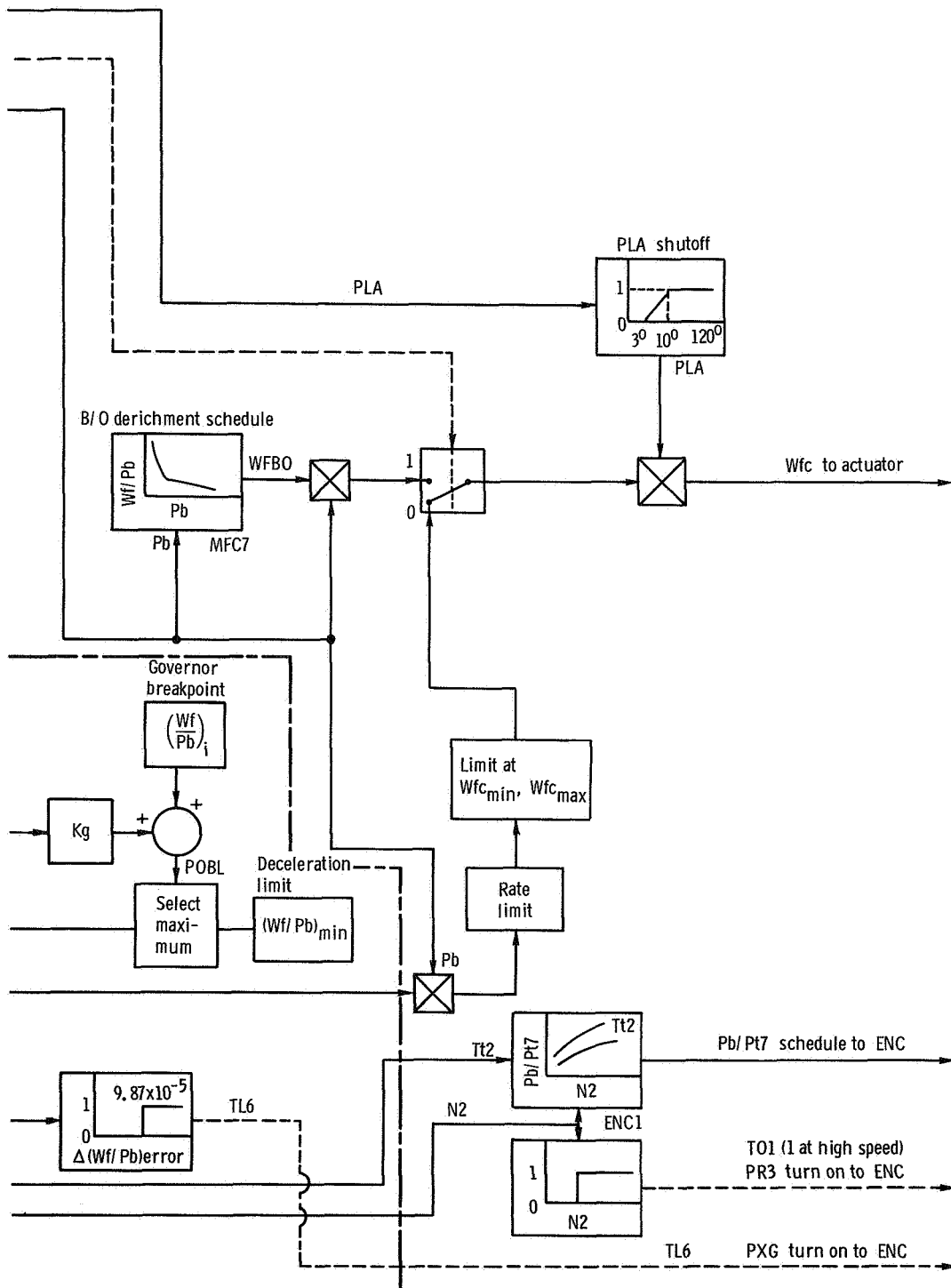
block diagram for TF30-P-3 engine.
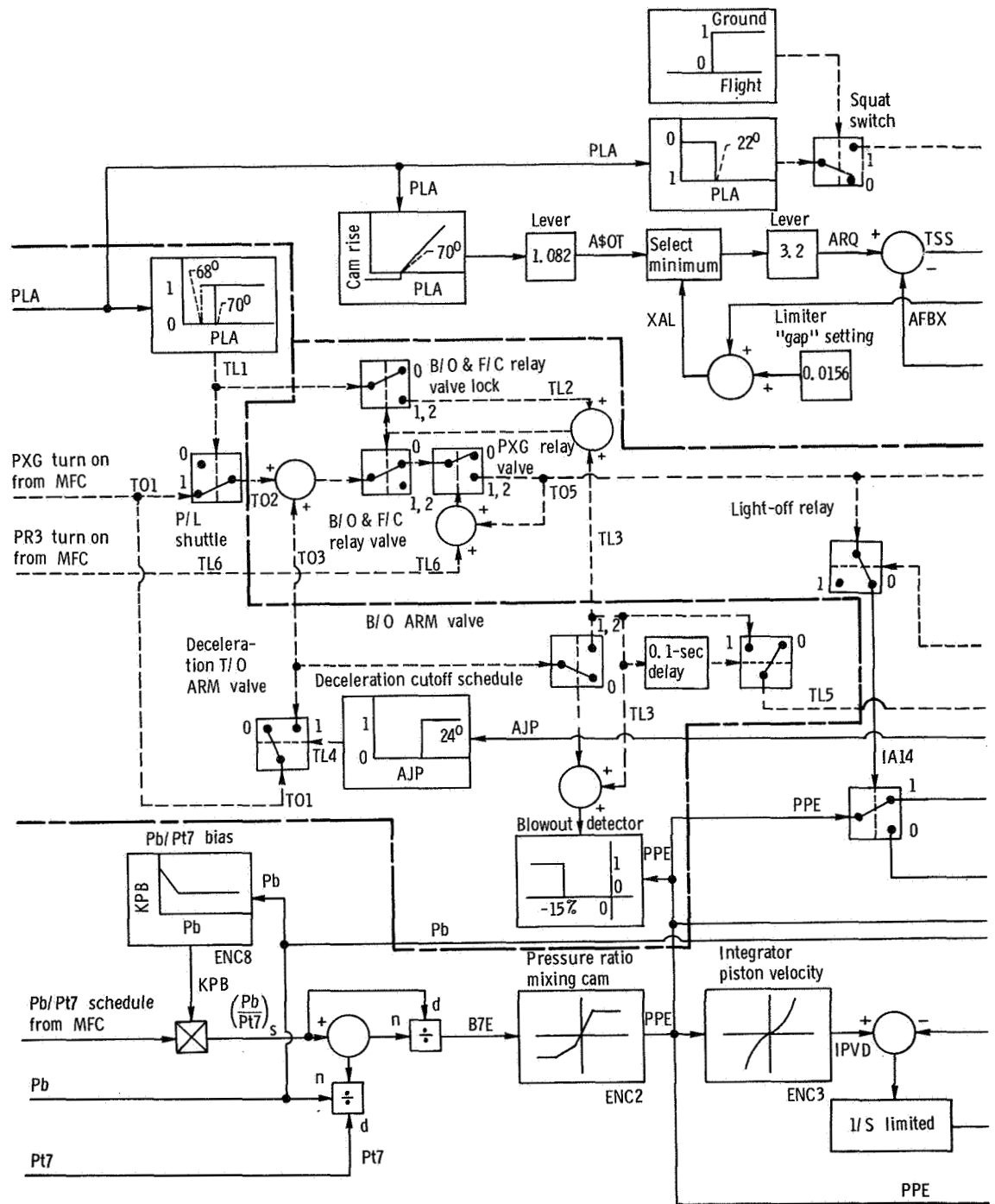
Figure 3. - Exhaust nozzle control
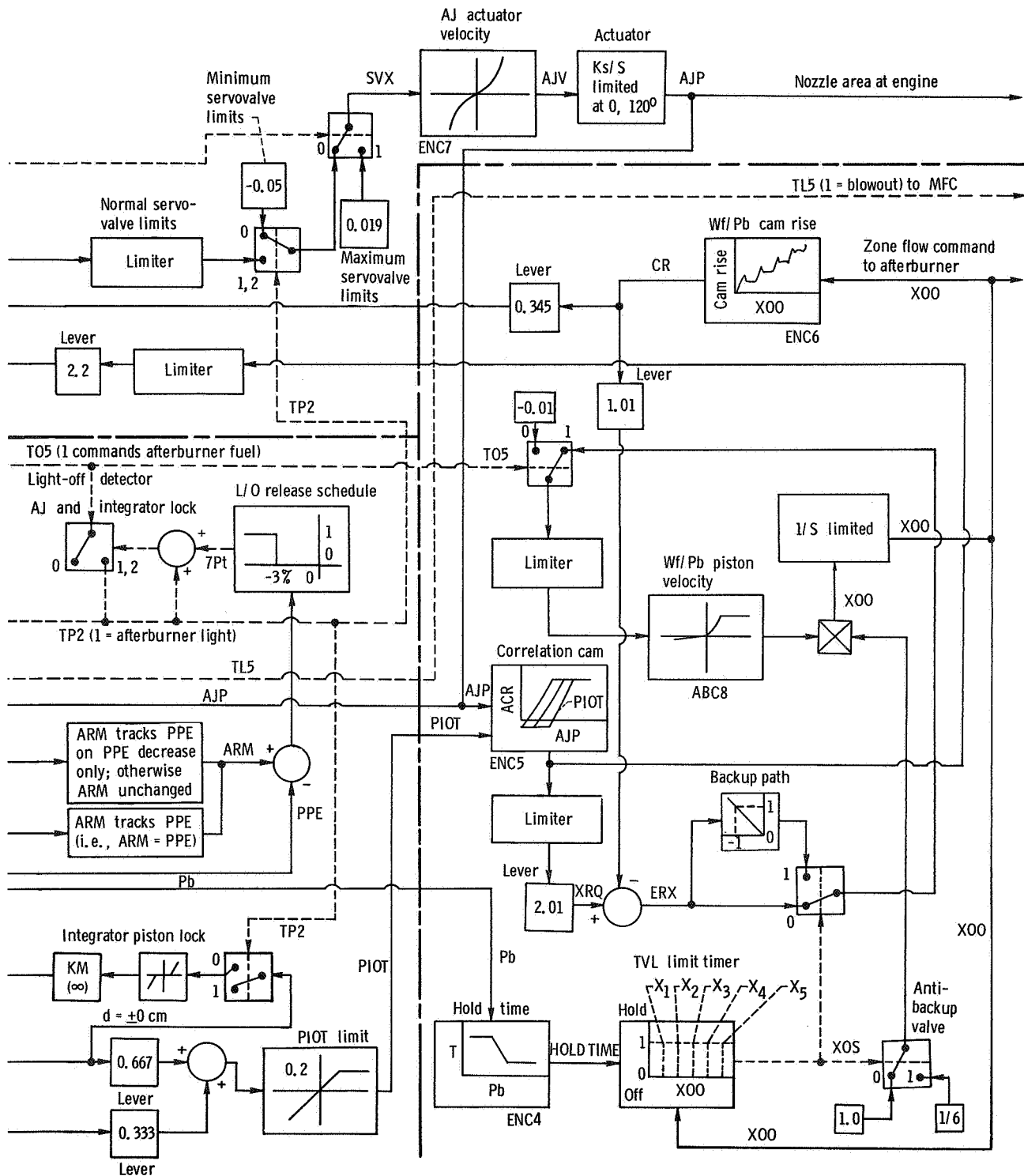
block diagram for TF30-P-3 engine.
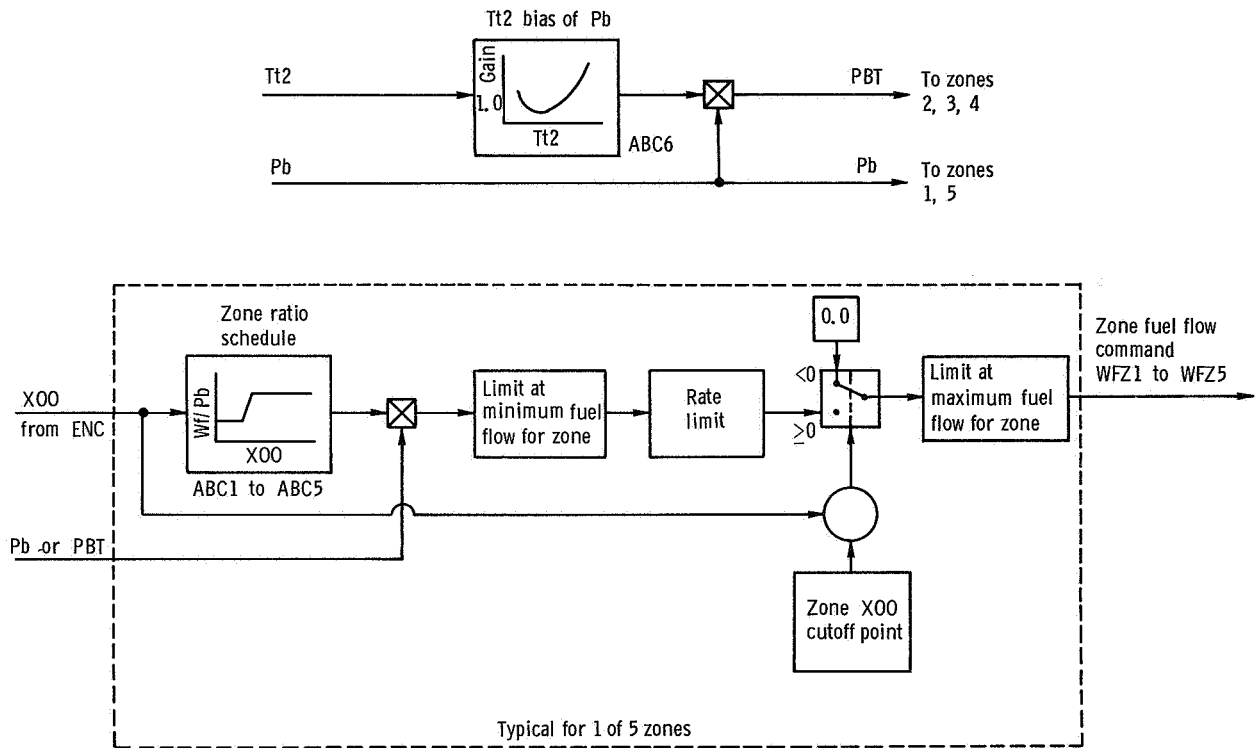
Figure 4. - Afterburner fuel control block diagram for TF30-P-3 engine.
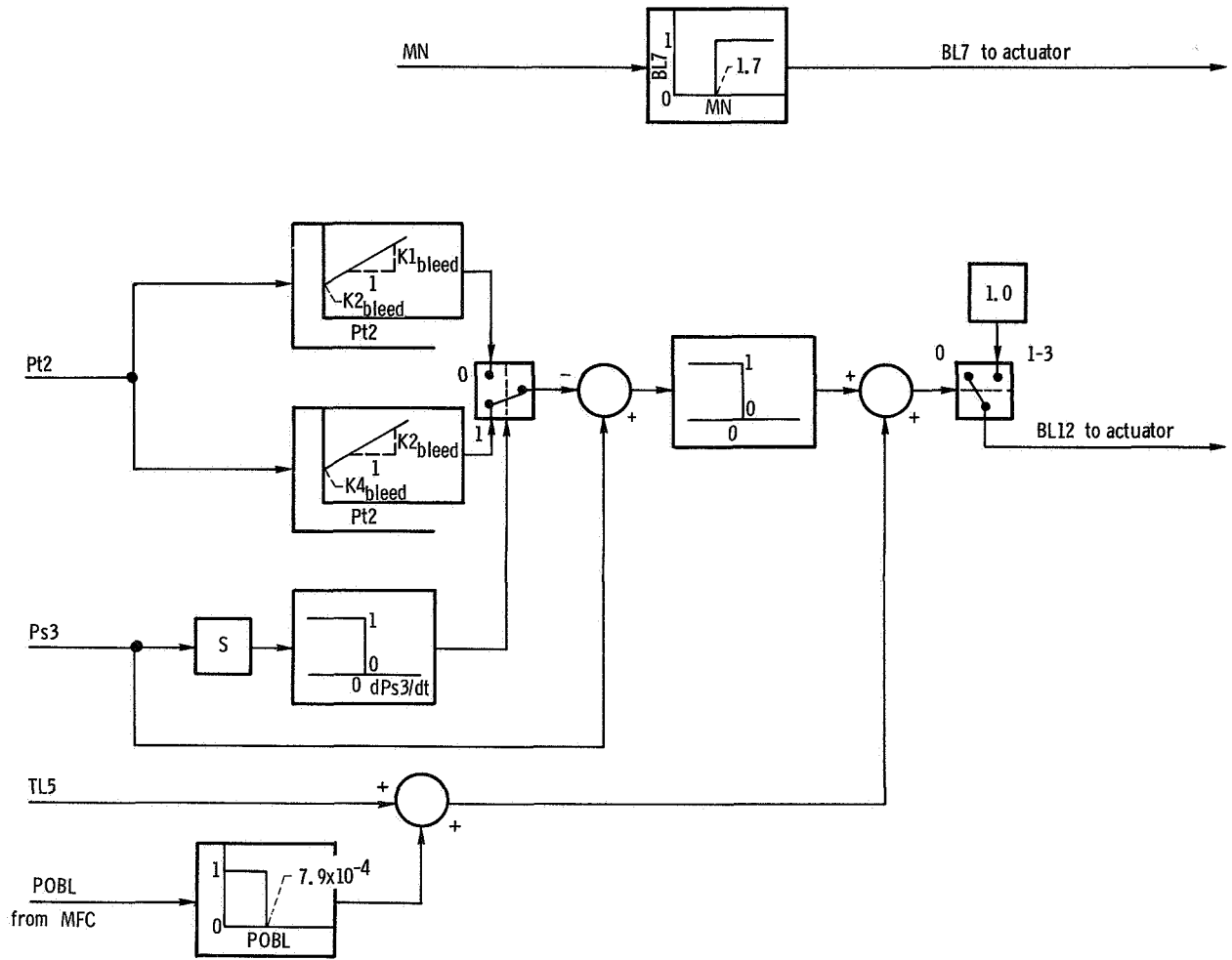
Figure 5. – Bleed door control block diagram.
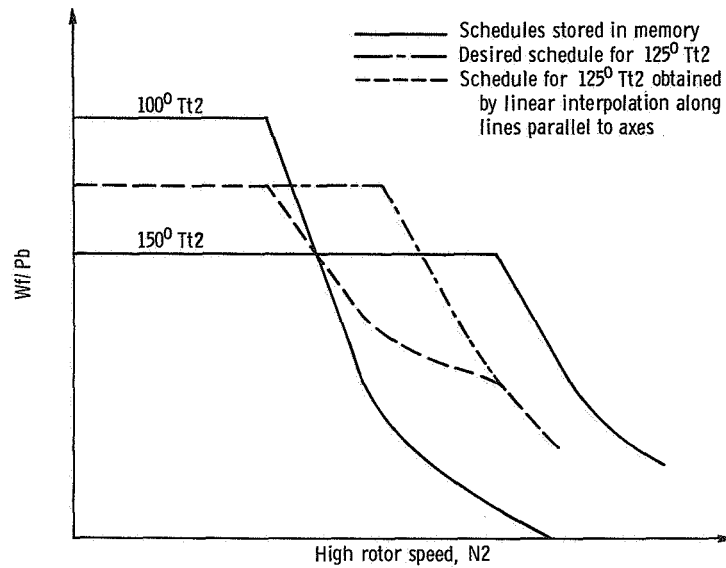
Figure 6. - Inaccuracy produced by using linear interpolation to generate functions of two variables. (Not to scale.)
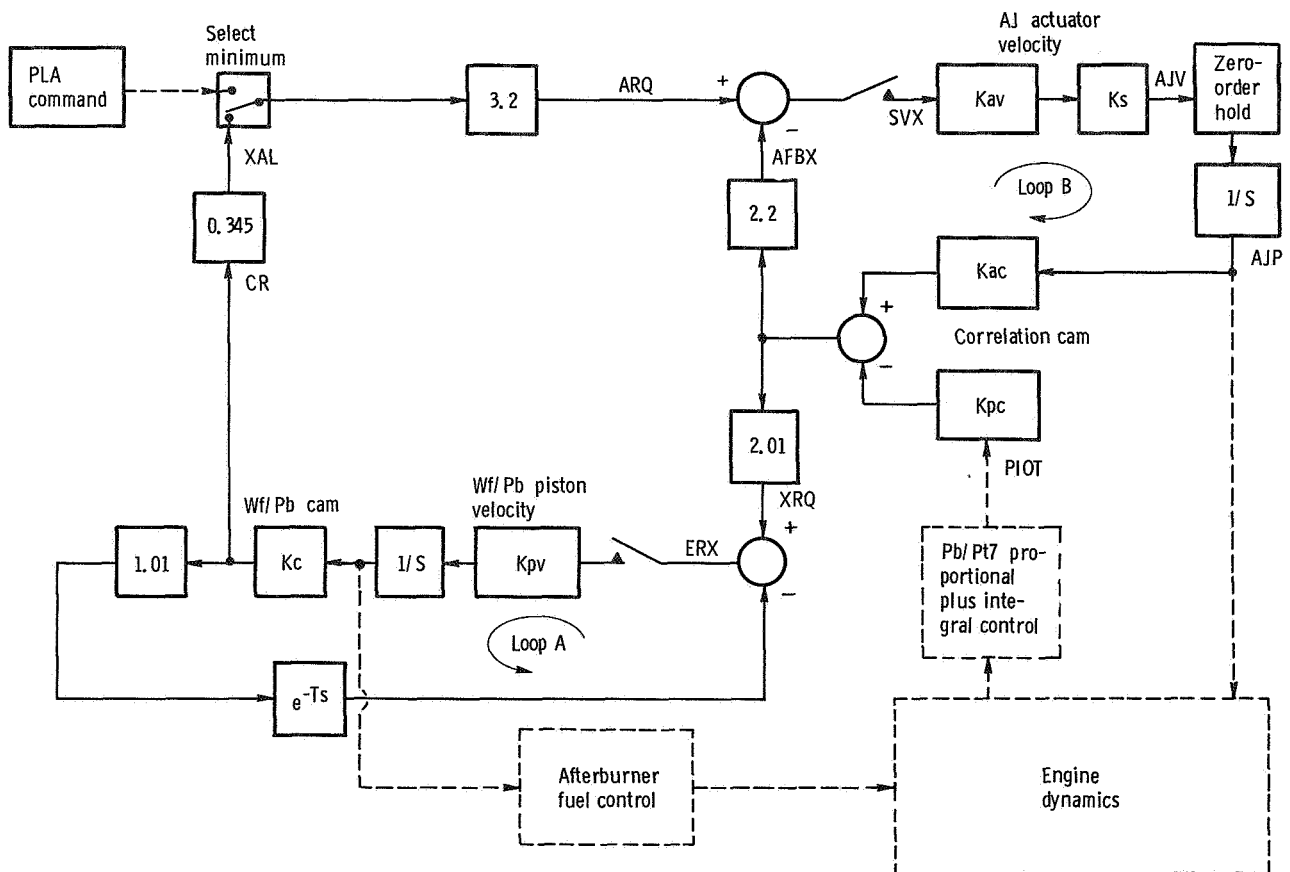
Figure 7. - Linearized model of exhaust nozzle control showing internal dynamic loops.
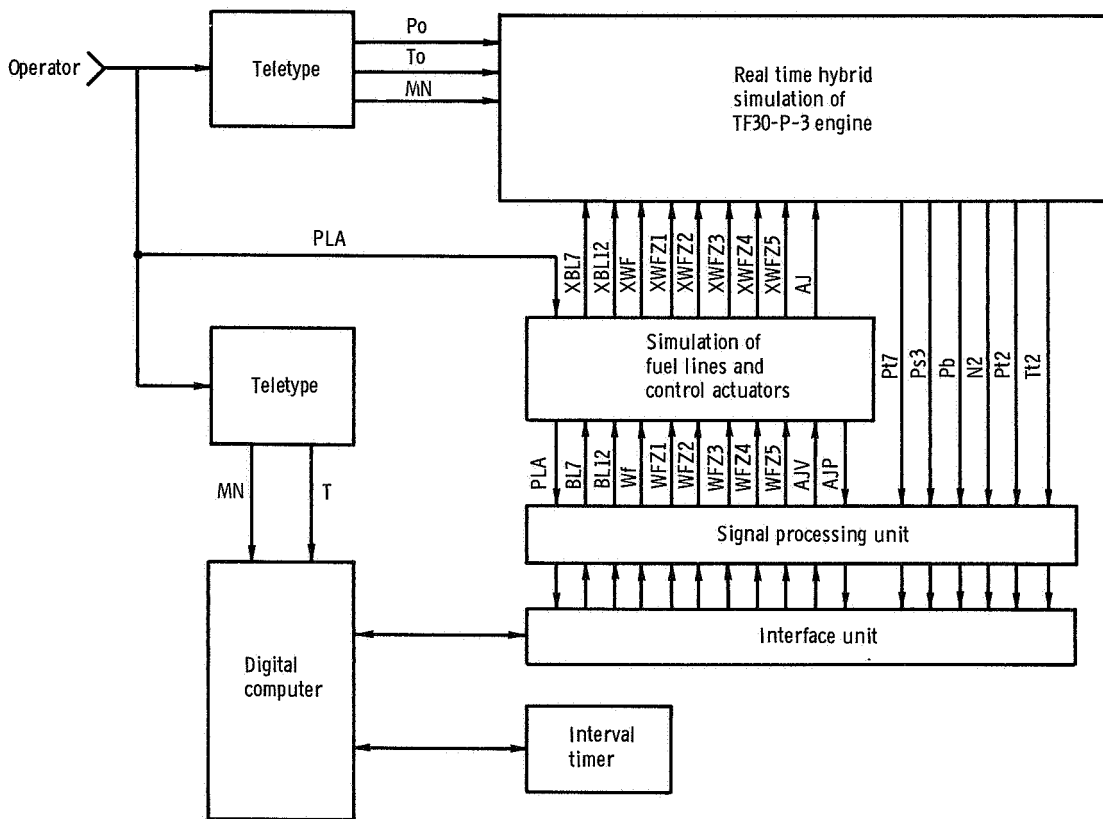
Figure 8. – Block diagram of configuration used to test digital control.
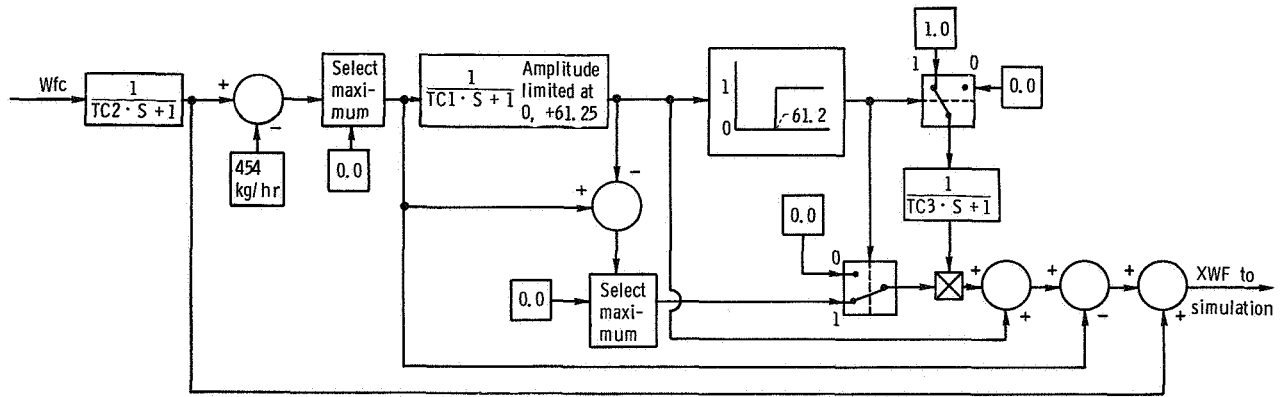
Main fuel line simulation
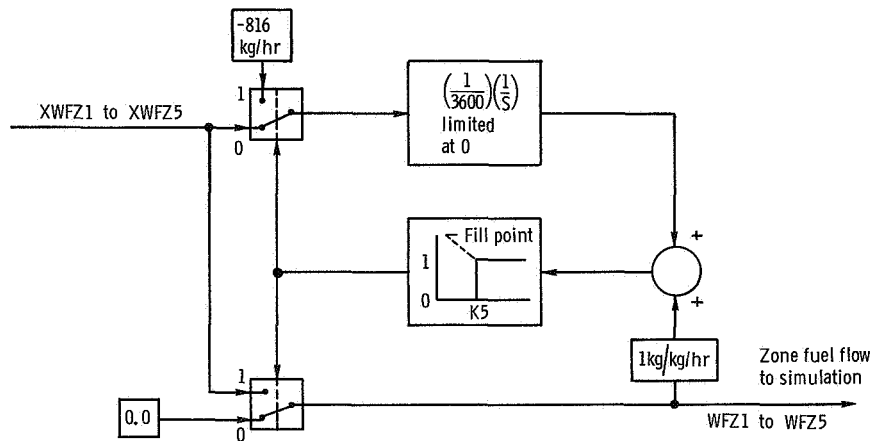
Afterburner fuel flow line fill simulation (typical for 1 of 5 zones)
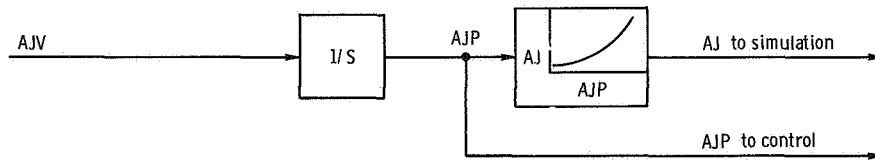
Exhaust nozzle position servo and area simulation
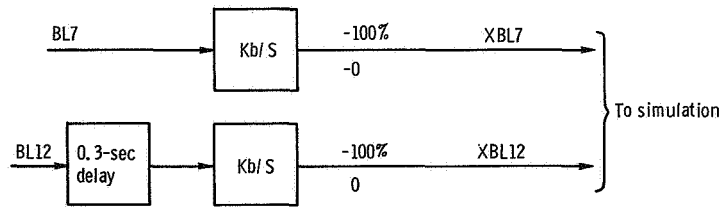
Bleed door simulation
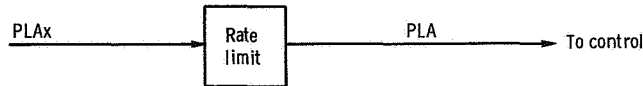
PLA rate limit

Figure 9. – Actuator simulation block diagram.

42
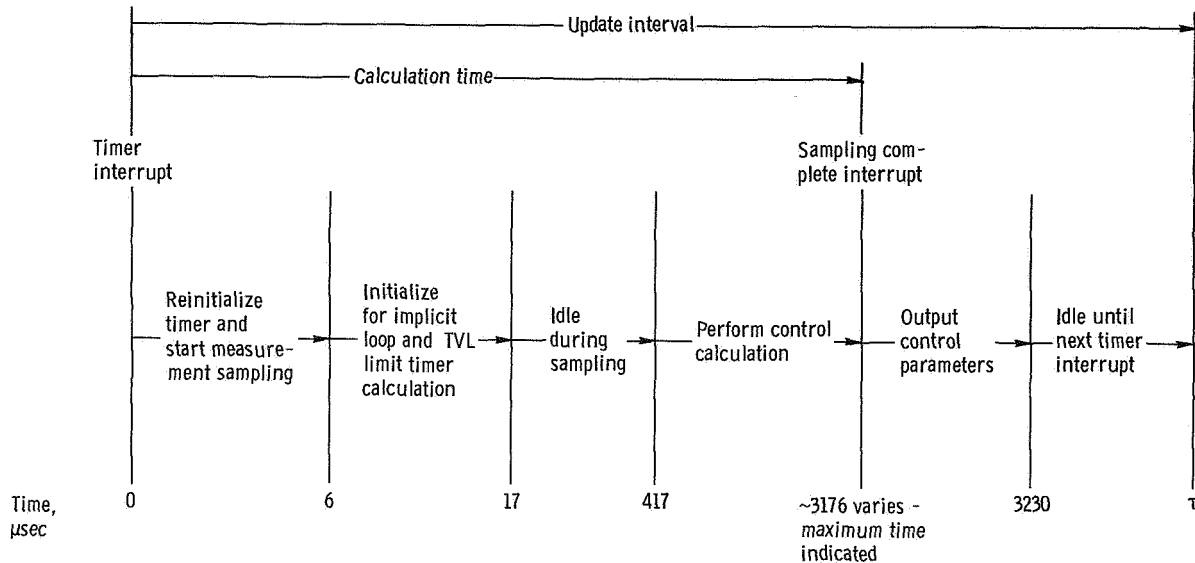
Figure 10. - Timing diagram for typical update interval. (When calculation time equals update interval, previous interval's calculation is output in 6- to 17-μsec interval, extending this interval by 54 μsec and the last two subintervals are eliminated.)
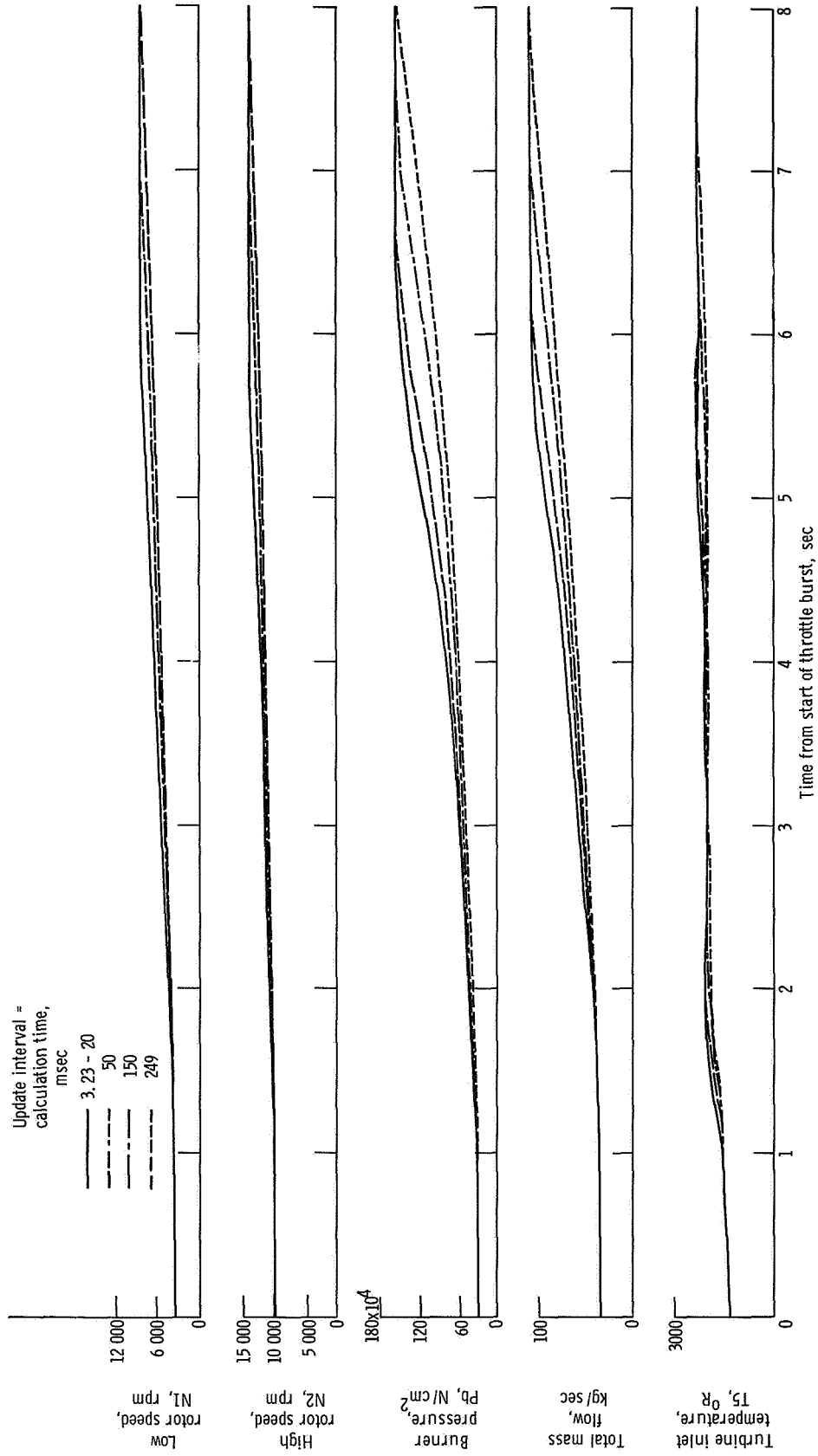
43
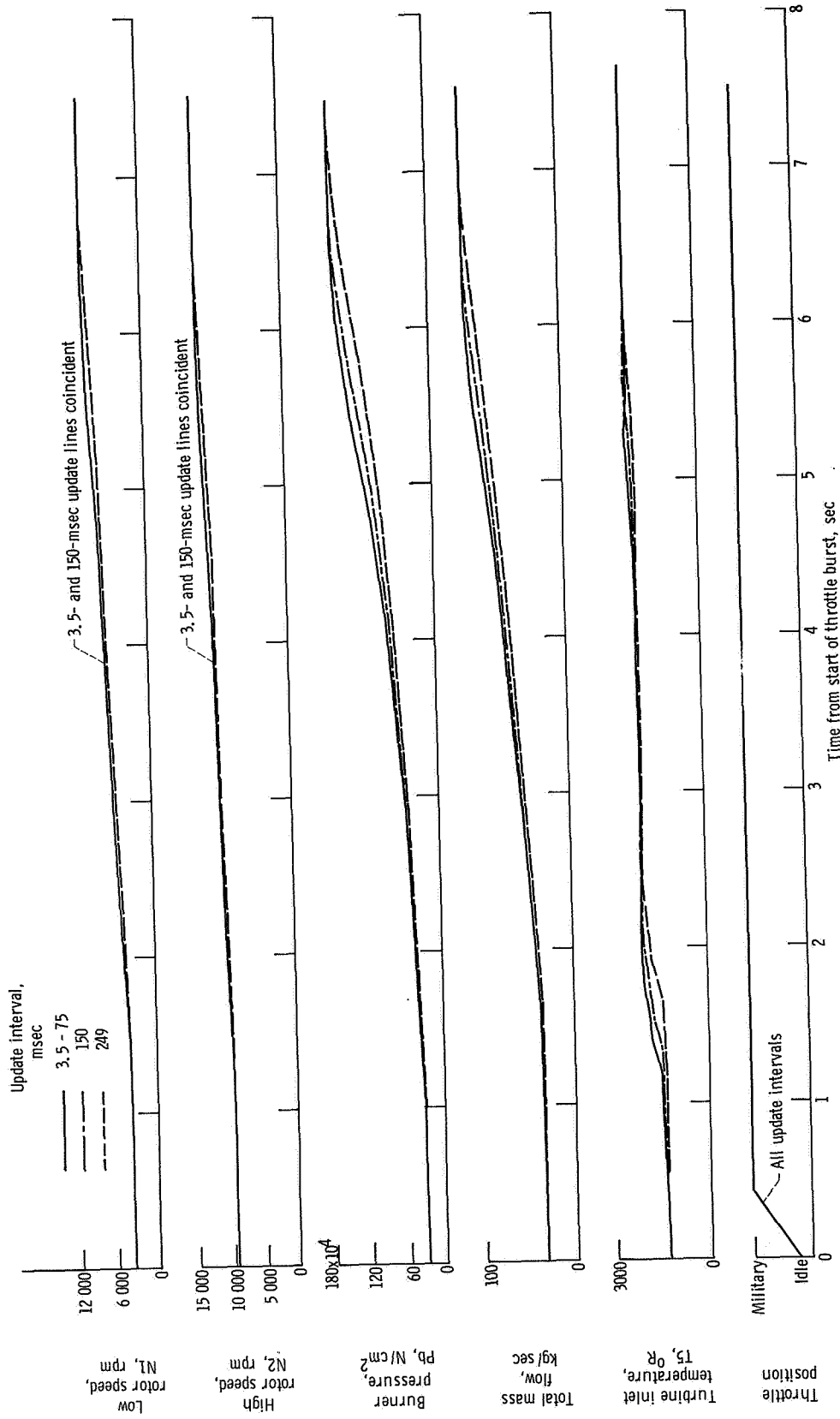
Figure 11. - Effects of update interval on simulated engine response for throttle burst from idle to military at sea-level static conditions.

44
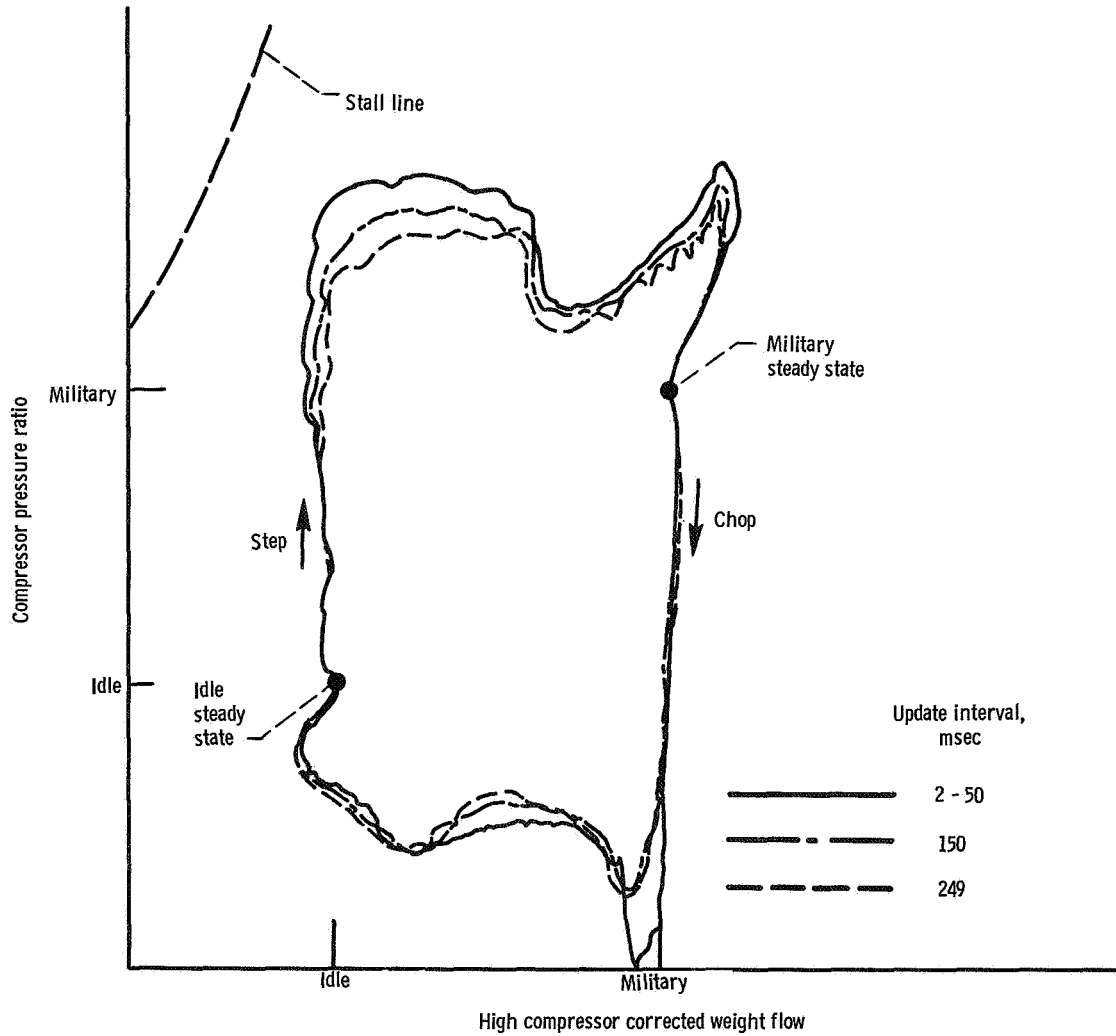
Figure 12. – Effects of update interval on high compressor pressure ratio for throttle steps and chops between idle and military.
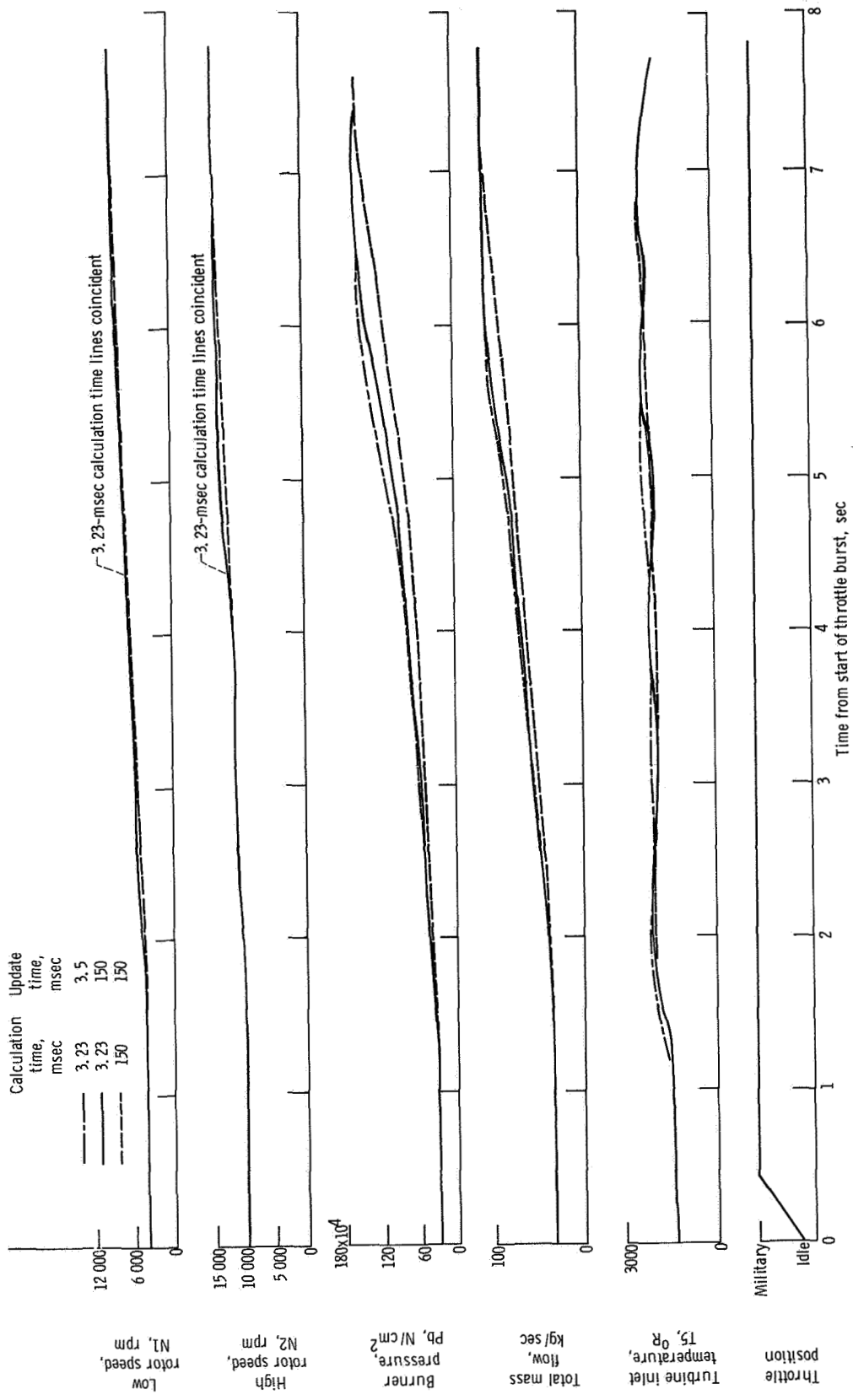
Figure 13. – Effect of increased calculation time on simulated engine response for throttle burst from idle to military.

46

Update interval =
calculation time,
msec

3.23 - 20
50
150
249

Low
rotor speed,
N1, rpm

12 000
6 000
0

High
rotor speed,
N2, rpm

15 000
10 000
5 000
0

Burner
pressure,
Pb, N/cm^2

180x10^4
120
60
0

Total mass
flow,
kg/sec

100
0

Turbine inlet
temperature,
T5, °R

3000
0

0   1   2   3   4   5   6   7   8

Time from start of throttle burst, sec

Figure 14. - Effects of extended calculation time and update interval on simulated engine response for throttle burst from idle to military at sea-level static conditions.
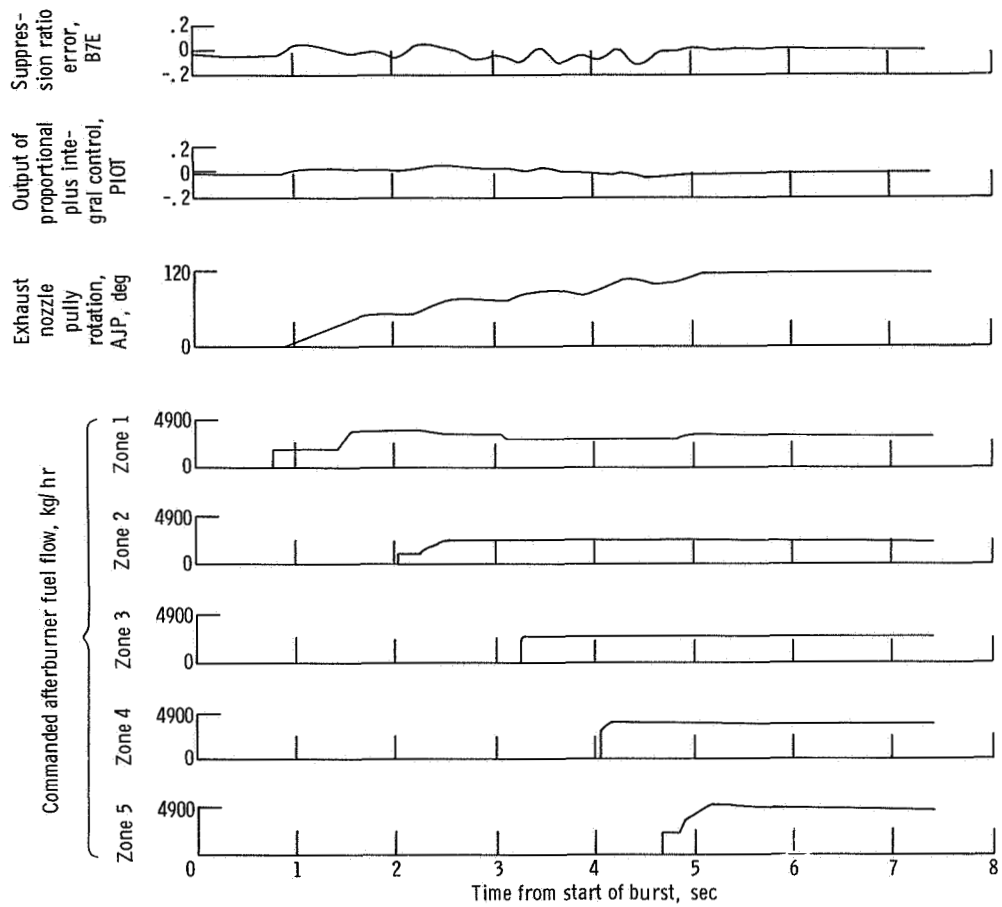
Figure 15. – Throttle burst from military to maximum for noniterative exhaust nozzle control using 3.5-msec update interval.

48

Suppres-
sion ratio
error,
B7E

.2
0
-.2

Output of
proportional
plus inte-
gral control,
P1OT

.2
0
-.2

Exhaust
nozzle
pully
rotation,
AJP, deg

120

0

Commanded afterburner fuel flow, kg/hr

Zone 1
4900
0
Oscillations caused by loop A instability

Zone 2
4900
0
Oscillations caused by loop A instability

Zone 3
4900
0

Zone 4
4900
0
Oscillations caused by loop A instability

Zone 5
4900
Oscillations caused by loop A instability

0   1   2   3   4   5   6   7   8
Time from start of burst, sec

Figure 16. – Throttle burst from military to maximum for noniterative exhaust nozzle control using 10-msec update interval.

49
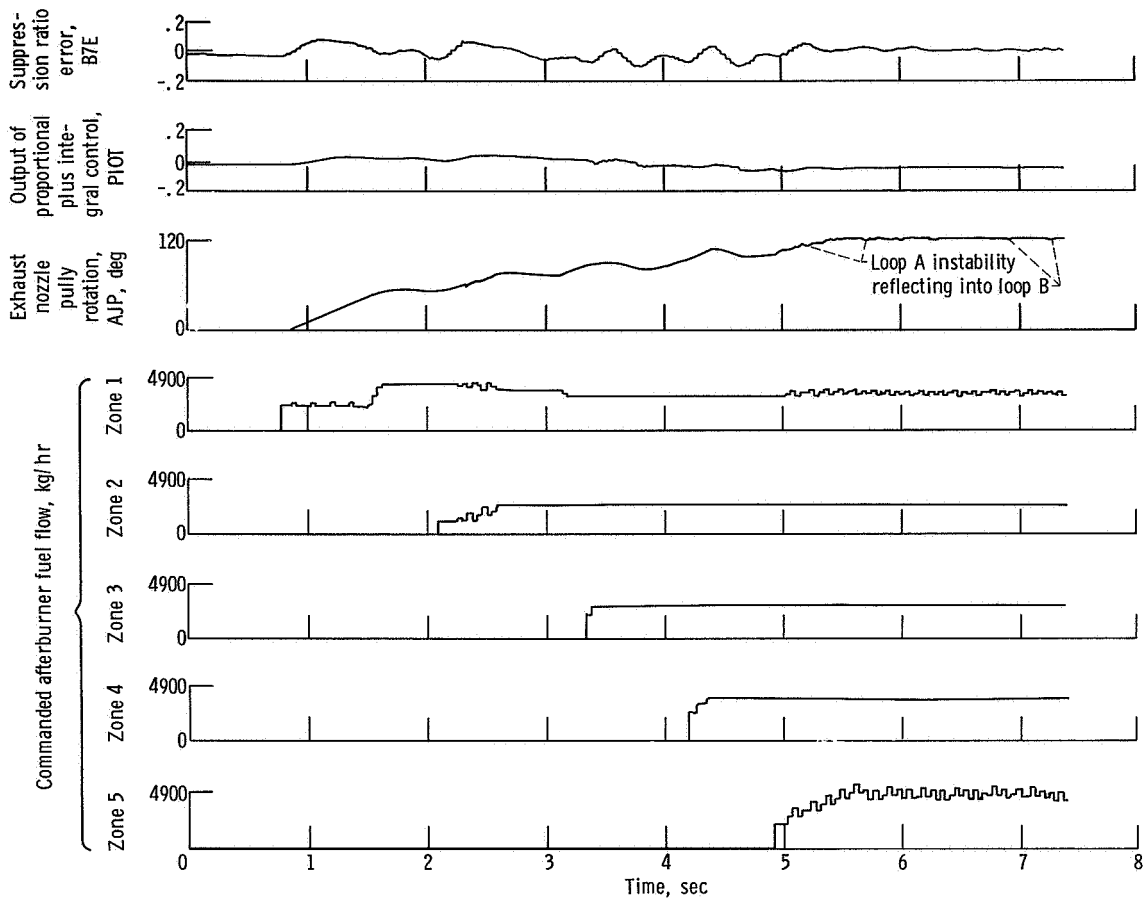
Figure 17. – Severe afterburner fuel flow oscillations caused by loop A instability to throttle burst from military to maximum for noniterative exhaust nozzle control using 40-msec update interval.

50
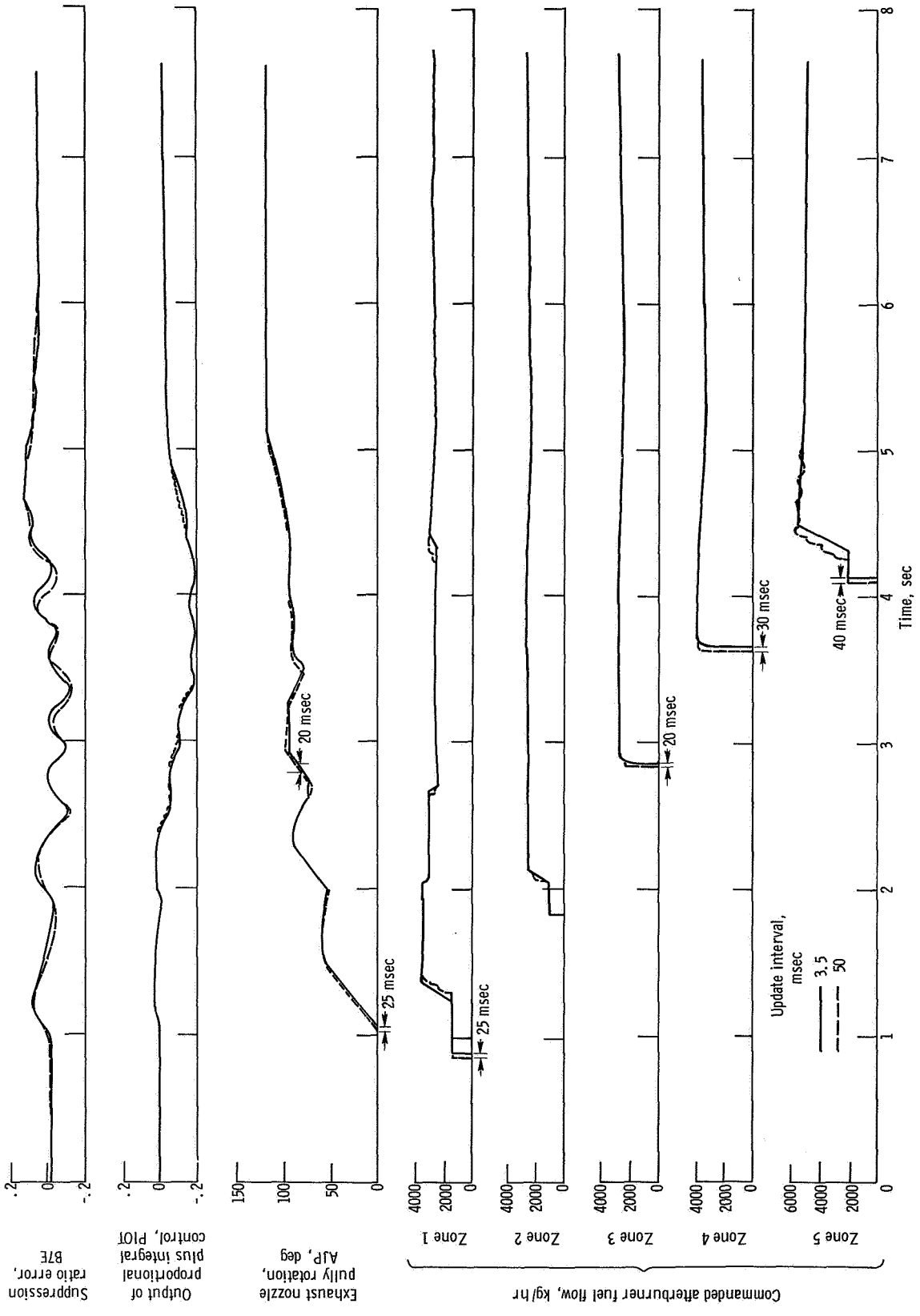
Figure 18. – Throttle burst from military to maximum for iterative exhaust nozzle control with acceptable control at 50-msec update interval.
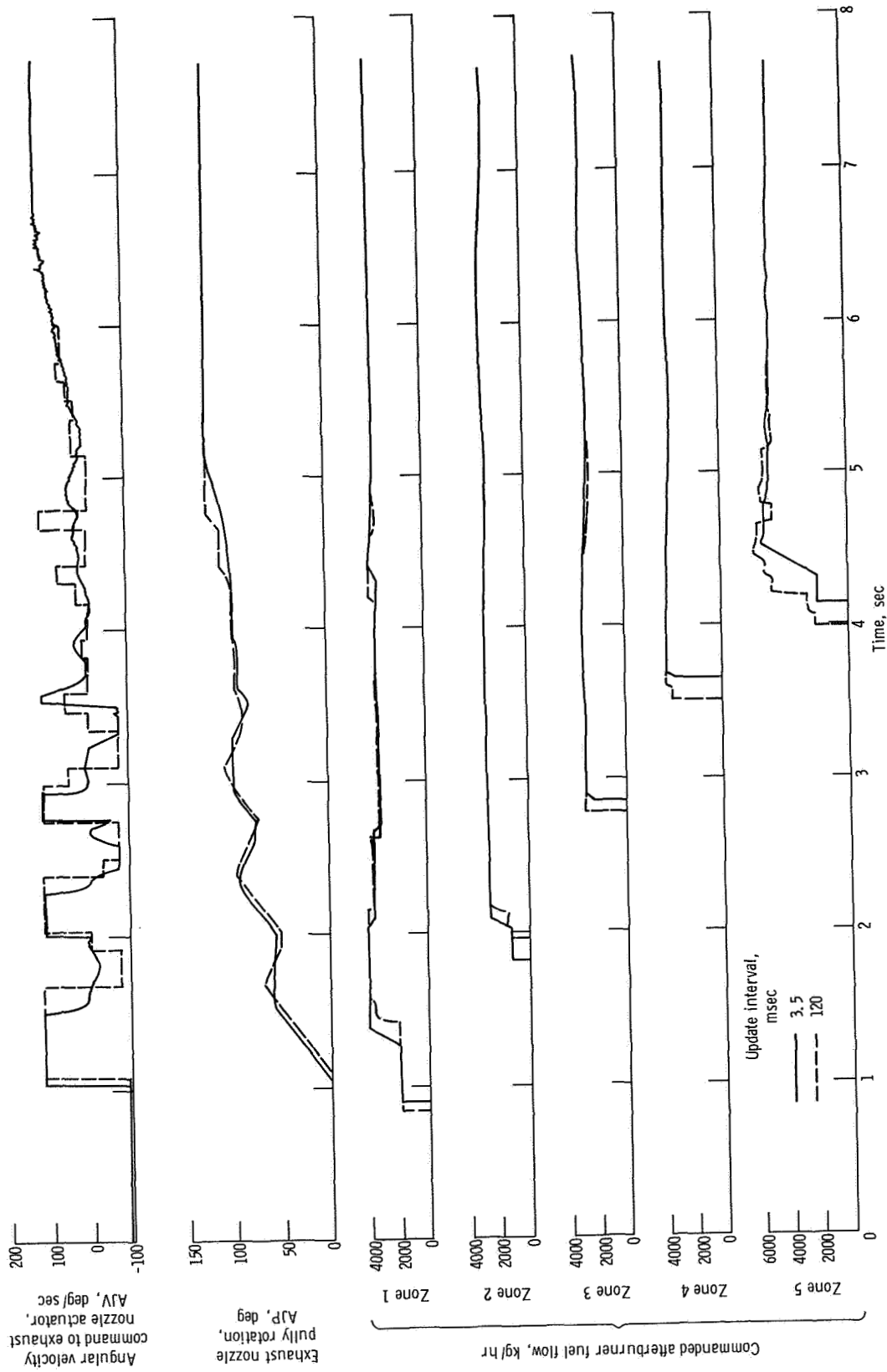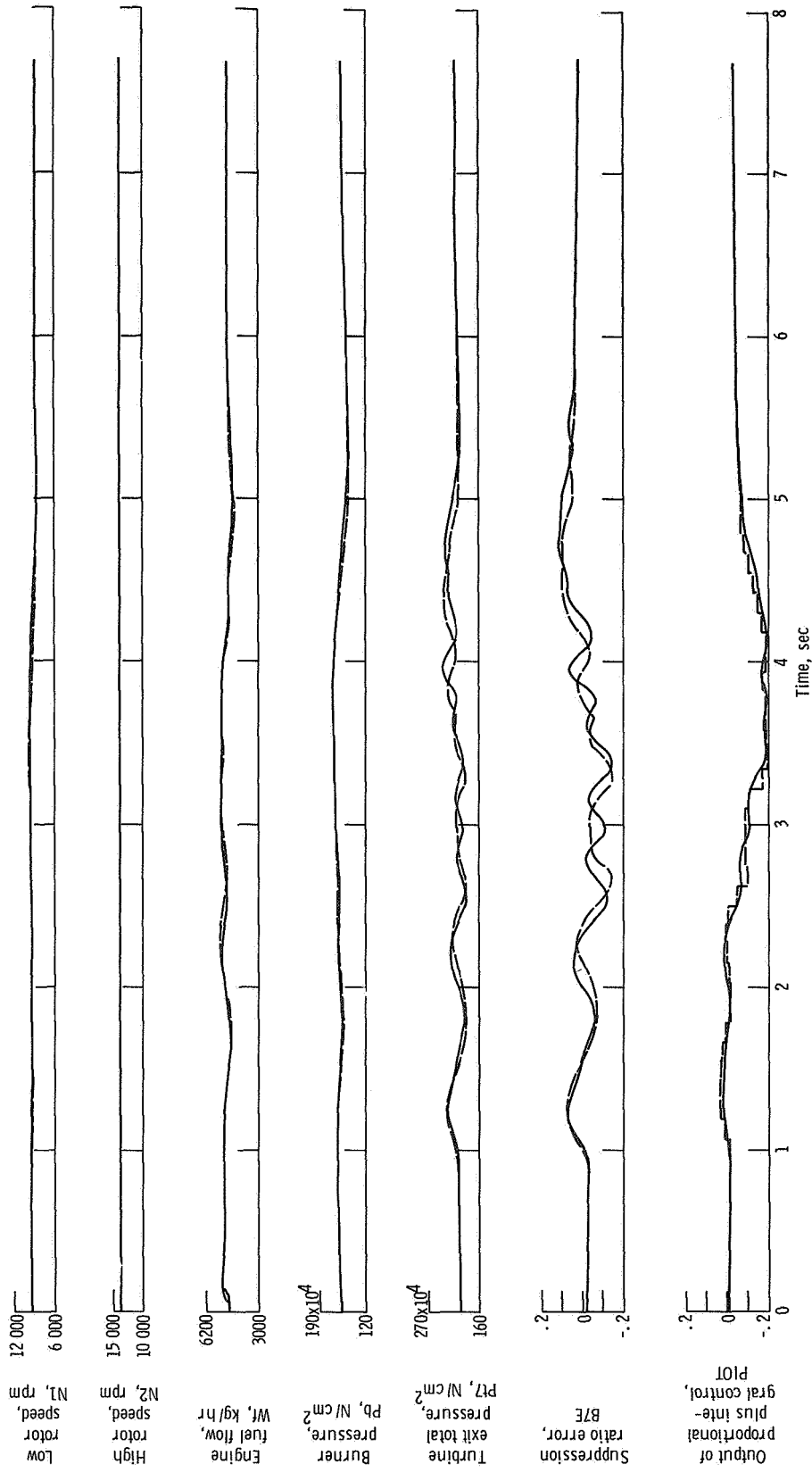
51

Figure 19. - Throttle burst from military to maximum for iterative exhaust nozzle control using 3.5- and 120-msec update interval.

52

Low
rotor
speed,
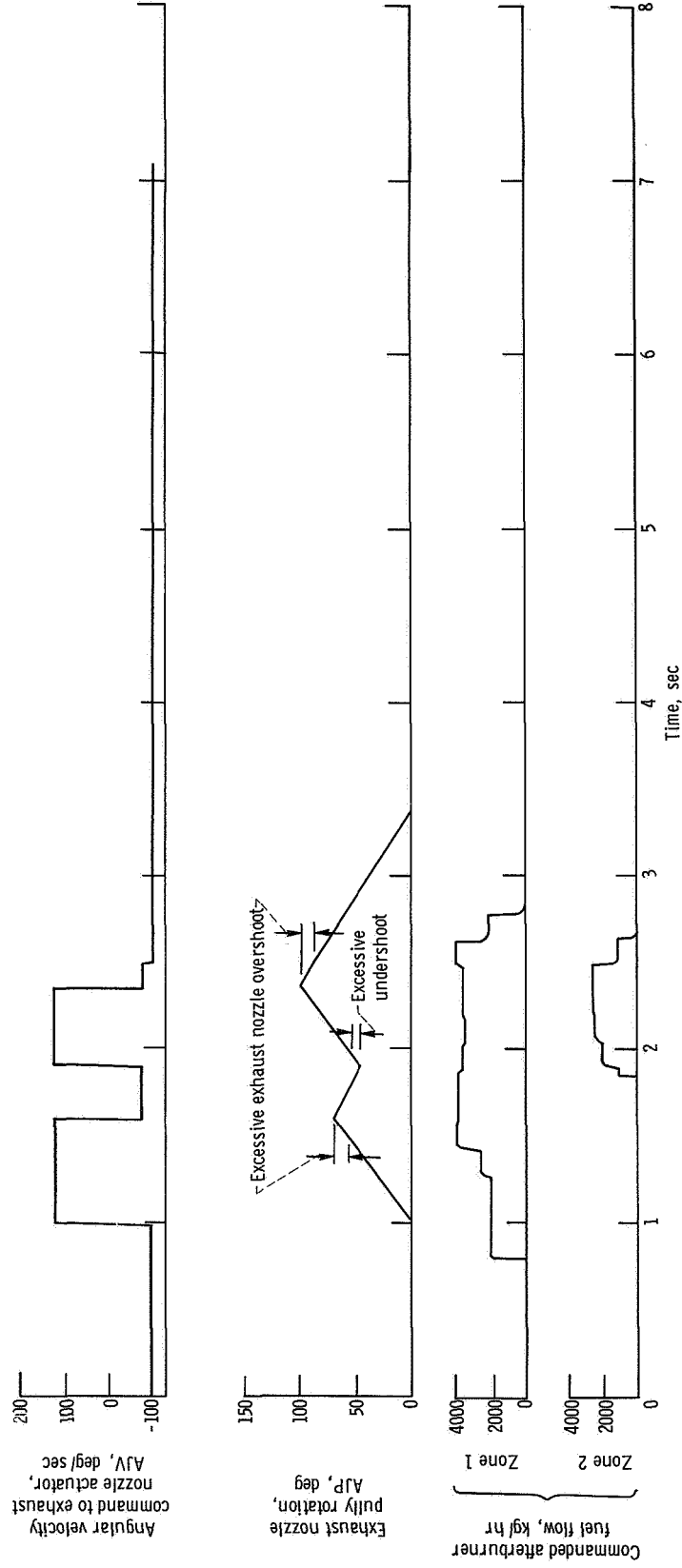N1, rpm

High
rotor
speed,
N2, rpm

Engine
fuel flow,
Wf, kg/hr

Burner
pressure,
Pb, N/cm^2

Turbine
exit total
pressure,
Pt7, N/cm^2

Suppression
ratio error,
B7E

Output of
proportional
plus inte-
gral control,
PI0T

12 000
6 000

15 000
10 000

6200
3000

190x10^4
120

270x10^4
160

.2
0
-.2

.2
0
-.2

0   1   2   3   4   5   6   7   8
Time, sec

Figure 19. - Concluded.

53

Figure 20. – Throttle burst from military to maximum for iterative exhaust nozzle control where 150-msec update interval caused false blowout detection and consequent failure to achieve afterburner operation.
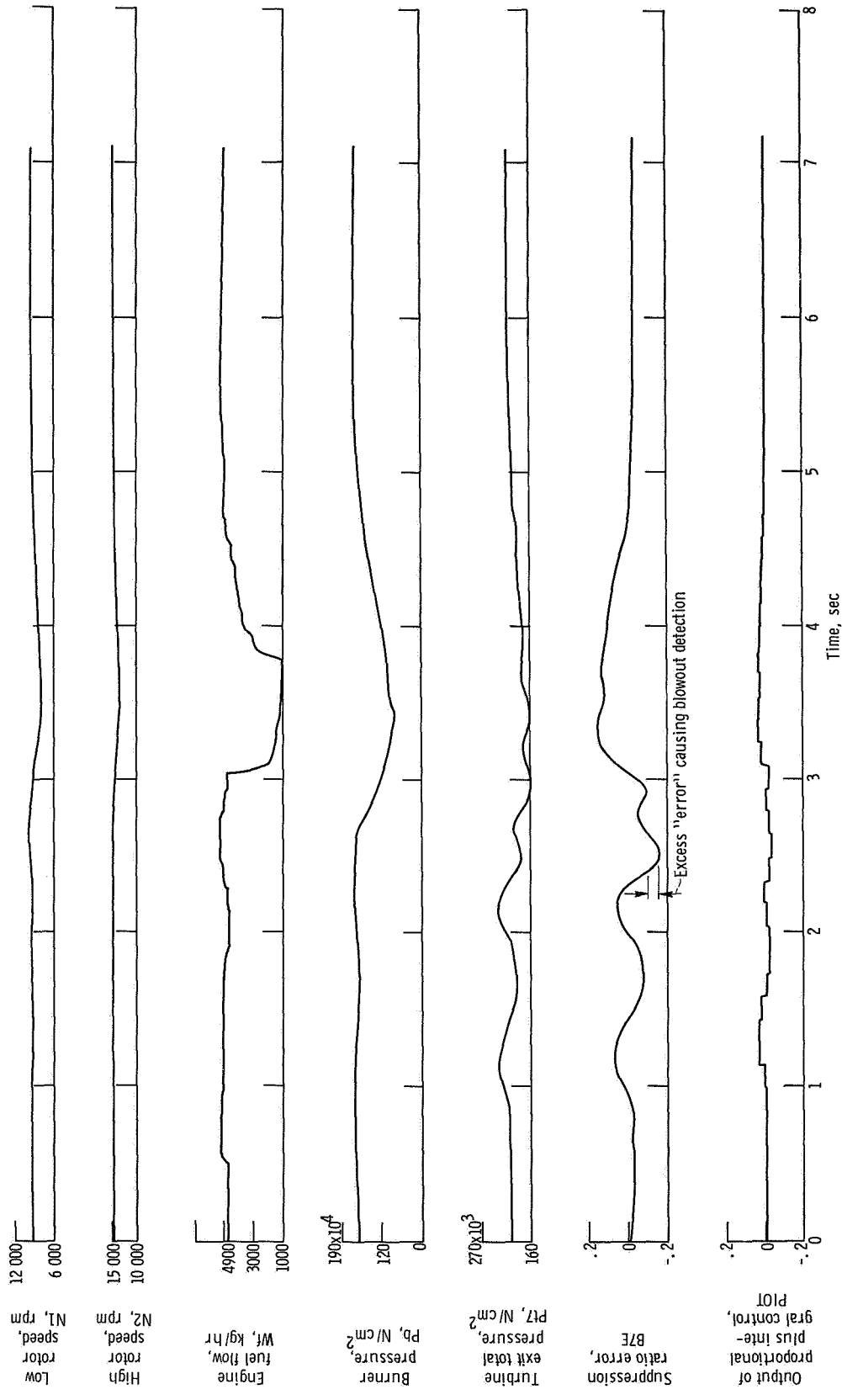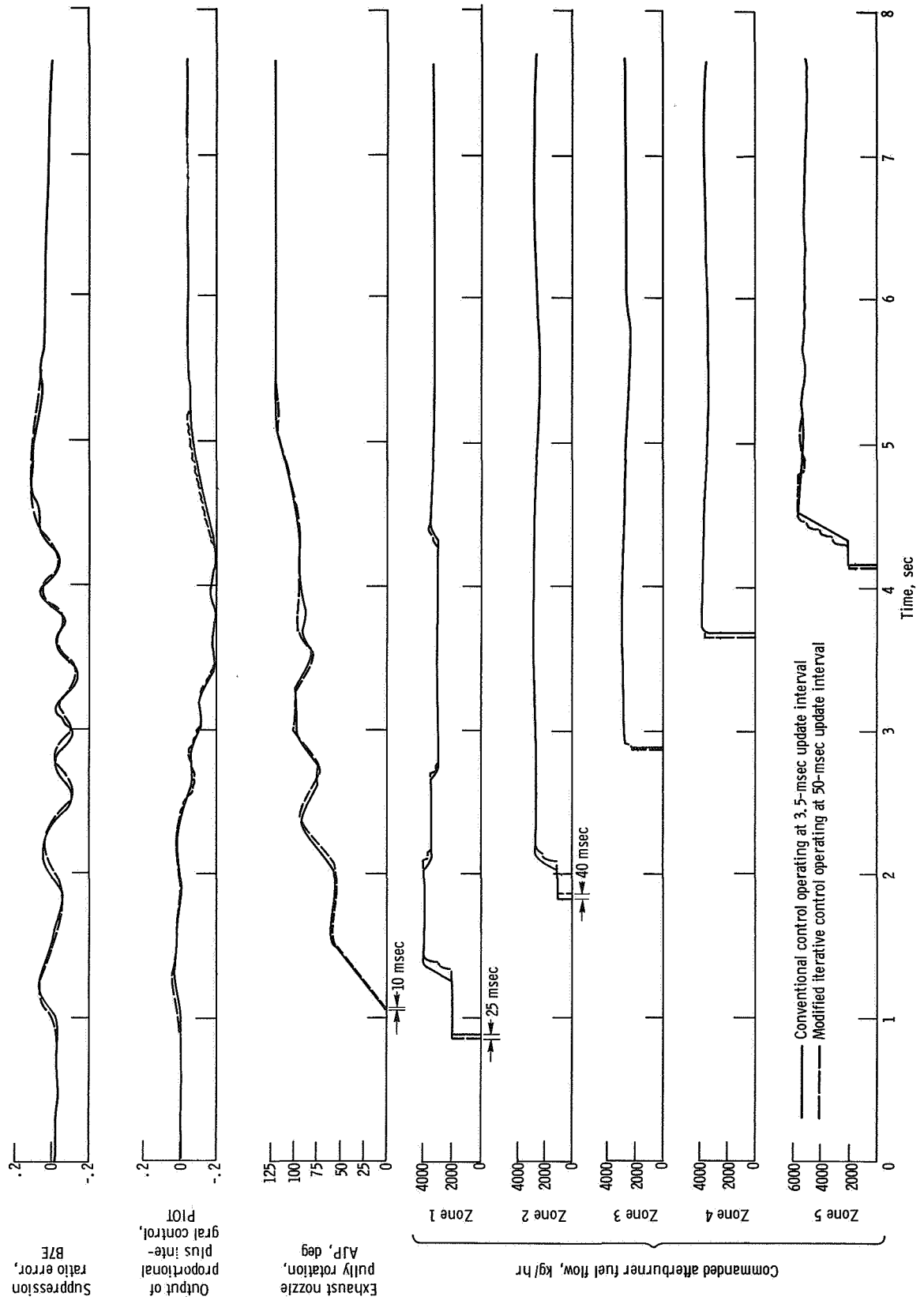
Figure 20. – Concluded.

Low rotor speed, N1, rpm

High rotor speed, N2, rpm

Engine fuel flow, Wf, kg/hr

Burner pressure, Pb, N/cm^2

Turbine exit total pressure, Pt7, N/cm^2

Suppression ratio error, B7E

Output of proportional plus integral control, PI0T

Time, sec

Excess "error" causing blowout detection

55

Suppression ratio error, B7E

Output of proportional plus inte-gral control, P10T

Exhaust nozzle pulley rotation, AJP, deg

Commanded afterburner fuel flow, kg/hr

Zone 1
Zone 2
Zone 3
Zone 4
Zone 5

10 msec

25 msec

40 msec

Conventional control operating at 3.5-msec update interval
Modified iterative control operating at 50-msec update interval

Time, sec

Figure 23. - Comparison of modified iterative control using external exhaust nozzle position servo to conventional control for throttle burst from military to maximum.
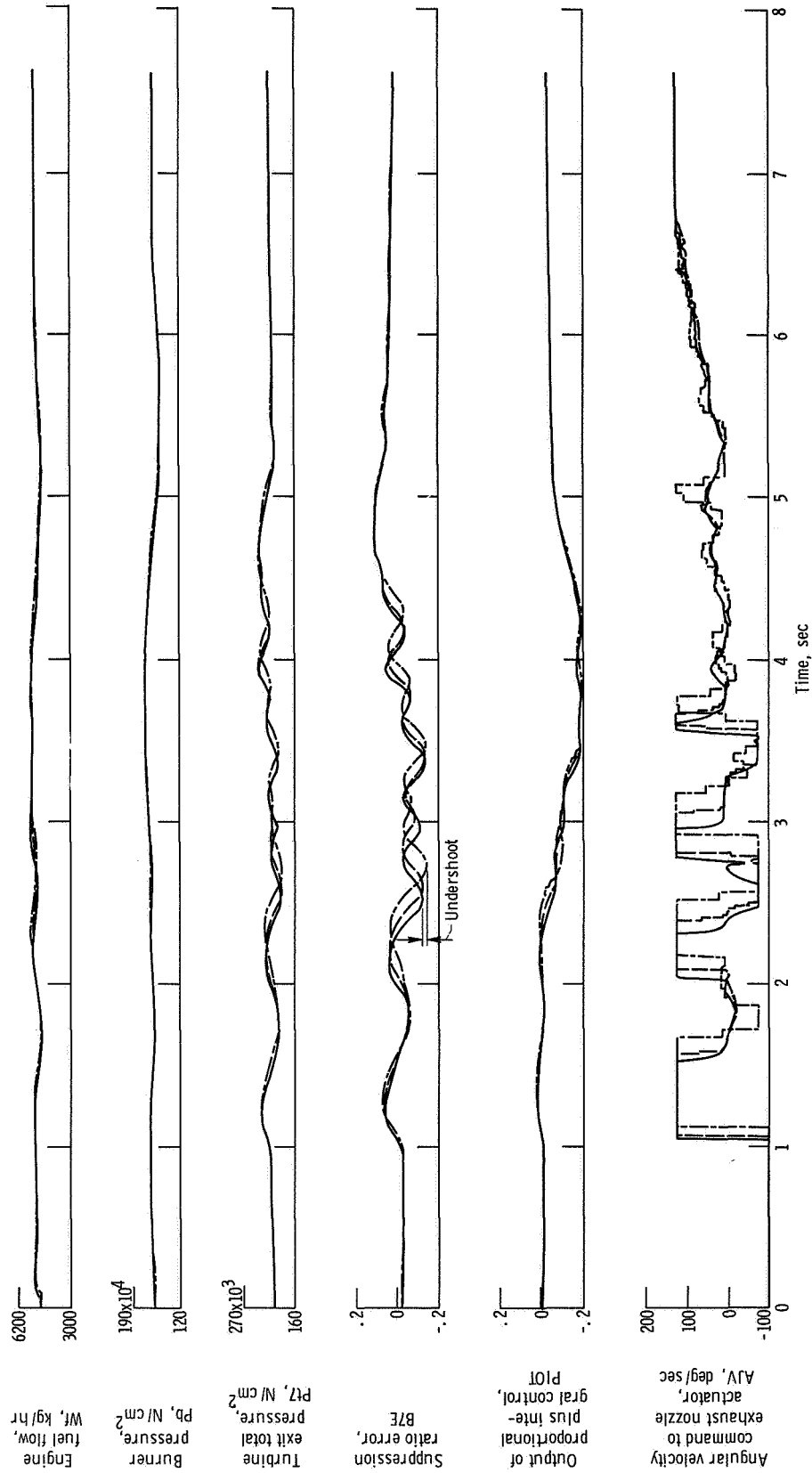
Figure 21. – Concluded.

57
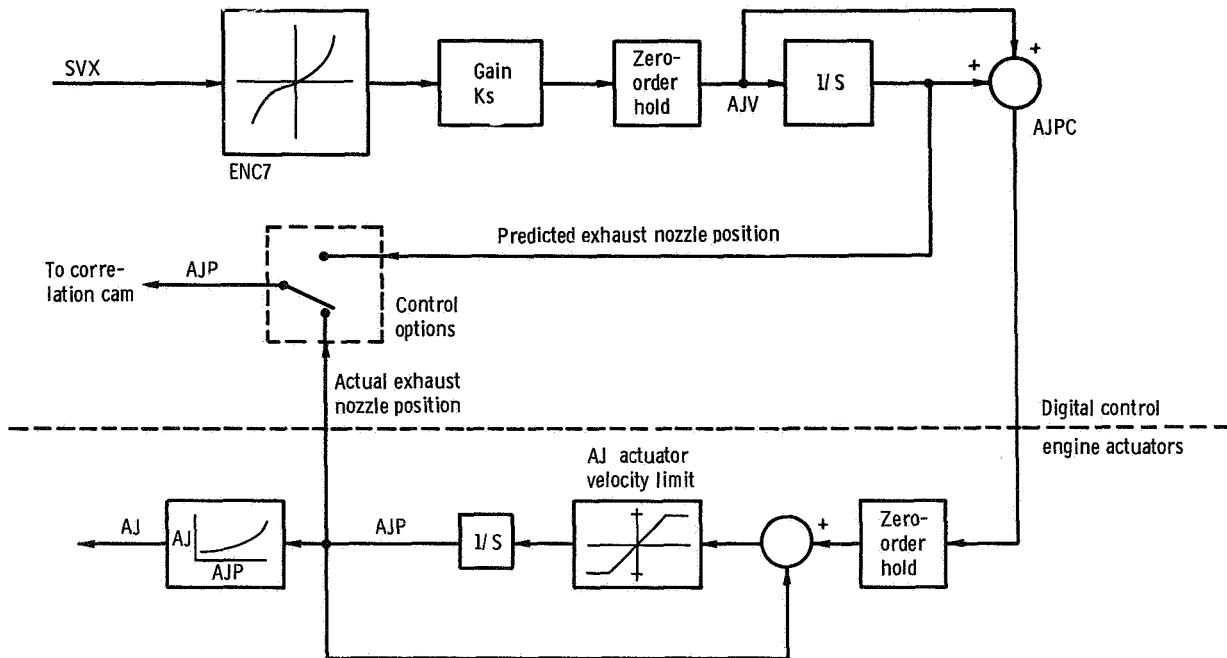
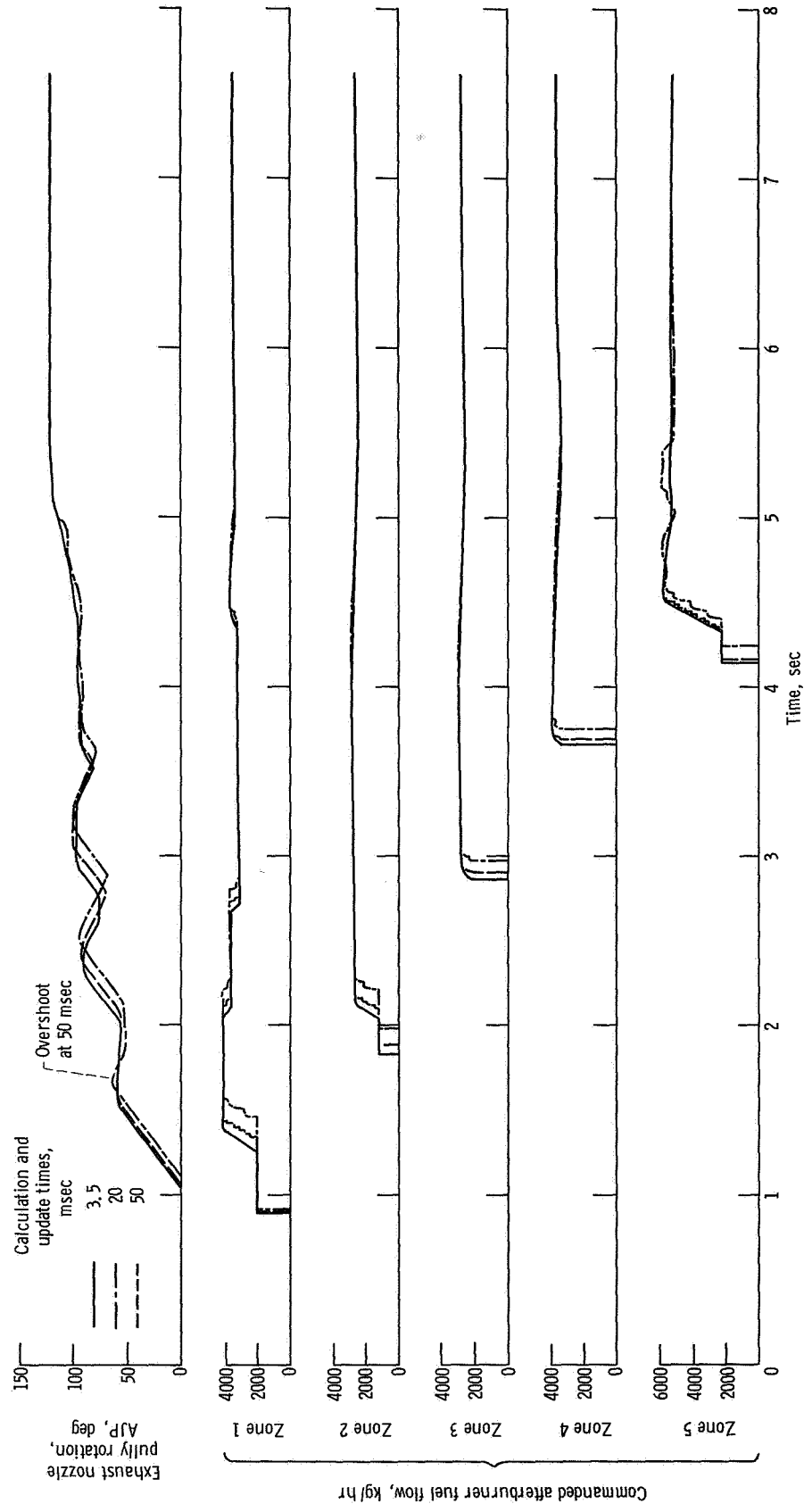Figure 22. – Block diagram of modified portion of exhaust nozzle control.

Figure 21. - Effects of increased calculation and update times on iterative exhaust nozzle control for throttle bursts from military to maximum.
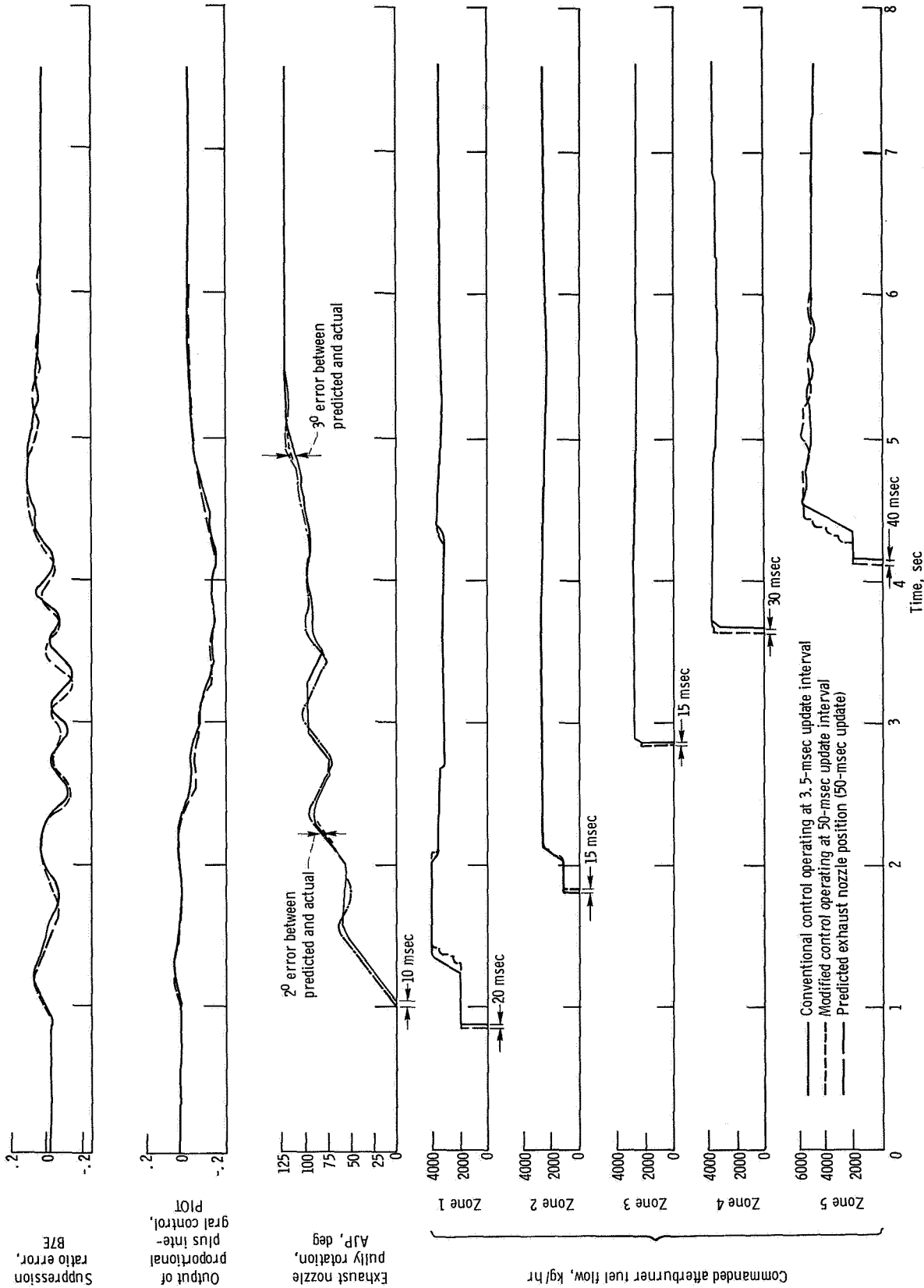
Figure 24. - Comparison of modified iterative control using external position servo and predicted exhaust nozzle position (in place of sampled position) to conventional control for throttle burst from military to maximum.

"The aeronautical and space activities of the United States shall be conducted so as to contribute . . . to the expansion of human knowledge of phenomena in the atmosphere and space. The Administration shall provide for the widest practicable and appropriate dissemination of information concerning its activities and the results thereof."

—NATIONAL AERONAUTICS AND SPACE ACT OF 1958

NASA SCIENTIFIC AND TECHNICAL PUBLICATIONS

TECHNICAL REPORTS: Scientific and technical information considered important, complete, and a lasting contribution to existing knowledge.

TECHNICAL NOTES: Information less broad in scope but nevertheless of importance as a contribution to existing knowledge.

TECHNICAL MEMORANDUMS: Information receiving limited distribution because of preliminary data, security classification, or other reasons. Also includes conference proceedings with either limited or unlimited distribution.

CONTRACTOR REPORTS: Scientific and technical information generated under a NASA contract or grant and considered an important contribution to existing knowledge.

TECHNICAL TRANSLATIONS: Information published in a foreign language considered to merit NASA distribution in English.

SPECIAL PUBLICATIONS: Information derived from or of value to NASA activities. Publications include final reports of major projects, monographs, data compilations, handbooks, sourcebooks, and special bibliographies.

TECHNOLOGY UTILIZATION PUBLICATIONS: Information on technology used by NASA that may be of particular interest in commercial and other non-aerospace applications. Publications include Tech Briefs, Technology Utilization Reports and Technology Surveys.

Details on the availability of these publications may be obtained from:

SCIENTIFIC AND TECHNICAL INFORMATION OFFICE

NATIONAL AERONAUTICS AND SPACE ADMINISTRATION
Washington, D.C. 20546